

AMERICAN UNIVERSITY OF BEIRUT

POSSIBLE CONTRIBUTION OF PERI-VASCULAR ADIPOSE  
THROMBO-INFLAMMATION TO CARDIAC AUTONOMIC  
NEUROPATHY: MODULATION BY RIVAROXABAN

by  
GHIDA SALIM AL ARAB

A thesis  
submitted in partial fulfillment of the requirements  
for the degree of Master of Science  
to the Department of Pharmacology and Toxicology  
of the Faculty of Medicine  
at the American University of Beirut

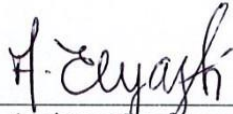
Beirut, Lebanon  
July 2021

AMERICAN UNIVERSITY OF BEIRUT

POSSIBLE CONTRIBUTION OF PERI-VASCULAR ADIPOSE  
THROMBO-INFLAMMATION TO CARDIAC AUTONOMIC  
NEUROPATHY: MODULATION BY RIVAROXABAN

by  
GHIDA SALIM AL ARAB

Approved by:



Dr. Ahmed El-Yazbi, Assistant Professor  
Department of Pharmacology and Toxicology, AUBFM

Advisor



Dr. Ramzi Sabra, Assistant Dean, Chairperson and Professor  
Department of Pharmacology and Toxicology, AUBFM

Member of Committee

Dr. Ali Eid, Assistant Professor  
Department of Pharmacology and Toxicology, AUBFM



Member of Committee

Dr. Fouad Zouein, Assistant Professor  
Department of Pharmacology and Toxicology, AUBFM



Member of Committee

Date of thesis defense: July 7, 2021

AMERICAN UNIVERSITY OF BEIRUT

THESIS RELEASE FORM

Student Name: AL Arab Ghida Salim  
Last First Middle

I authorize the American University of Beirut, to: (a) reproduce hard or electronic copies of my thesis; (b) include such copies in the archives and digital repositories of the University; and (c) make freely available such copies to third parties for research or educational purposes:

- As of the date of submission
- One year from the date of submission of my thesis.
- Two years from the date of submission of my thesis.
- Three years from the date of submission of my thesis.

Ghida 16/8/2021  
Signature Date

## ACKNOWLEDGEMENTS

As a start, I would like to thank my supervisor Dr. Ahmed El-Yazbi for all the support he provided me with during this hard period. Throughout all the obstacles we were facing, Dr. Ahmed was always there pushing me forward, ensuring that I get to learn each technique and detail, and bearing my diversified persistent questions. Thank you for being the best mentor anyone could ask for.

I am also thankful to the chairman Dr. Ramzi Sabra, Dr. Ali Eid, and Dr. Fouad Zouein for agreeing to be members of my thesis committee, and for always being around providing their professional support and motivation.

A warm thanks to my lab mates who became my second family. Thank you for providing me with your technical and emotional support during the past overwhelming days, and for being part of this accomplishment. Thanks to Mrs. Nahed Mougharbil, Rana Alaaeddine, Nour Bakkar, Aya Al Saidi, Haneen Dwaib, Safaa Hammoud, Ibrahim Zaim, Alaa Ghazi, Baraa Hamzeh, Ghina Ajouz, Rana Ghazi, Sarah El Meski and Housam Koussa.

A special thanks goes to my friends and cousins who managed to tolerate my continuous nagging through the past two years.

Finally, with tears in my eyes, I would like to thank my family who I honor this accomplishment to. Thank you for always being there, through my ups and downs. You never failed to make me smile and I am grateful for having a family like you! I promise to always make you proud.

# ABSTRACT OF THE THESIS OF

Ghida Salim AL Arab

for

Master of Science

Major: Pharmacology and Toxicology

Title: Possible Contribution of Peri-vascular Adipose Thrombo-inflammation to Cardiac Autonomic Neuropathy: Modulation by Rivaroxaban

Cardiac autonomic neuropathy (CAN) is an early occurrence in type 2 diabetes (T2D) patients that represents a silent cause of cardiovascular mortality and morbidity. The pathophysiology of CAN is poorly understood however, the high prevalence of CAN in patients newly diagnosed with T2D suggests that its pathophysiology is rooted in an earlier stage of metabolic derangement, possibly being prediabetes. Our laboratory recently showed that prediabetes is associated with localized perivascular adipose tissue (PVAT) inflammation with a paracrine cardiovascular involvement, and sympathovagal imbalance leading to parasympathetic CAN. Literature reported that adipose inflammation is also associated with a rise in thrombin and factor Xa activity. Moreover, factor Xa-driven protease-activated receptor stimulation exacerbates inflammation provoking a continuous cycle.

In this present study, we intend to examine whether suppression of factor Xa activity in a prediabetic rat model will ameliorate the localized PVAT inflammation. This will be associated with improved cardiac autonomic function, as well as reversal of cardiovascular structural abnormalities.

A non-obese prediabetic rat model was used. Sprague-Dawley rats were fed a mild hypercaloric diet for twelve weeks to induce PVAT inflammation. In vivo invasive hemodynamic measurement of the baroreflex sensitivity showed reduced parasympathetic activity in prediabetic rats that was reversed by rivaroxaban treatment. After sacrifice, PVAT inflammation was observed as an increased interleukin-1 $\beta$  expression, adipocyte hypertrophy, and increased oxidative stress, ameliorated by rivaroxaban treatment. Similarly, increased cardiac and brainstem oxidative stress were noted in prediabetic rats where only cardiac oxidative stress was reversed by rivaroxaban treatment.

Rivaroxaban was shown to have no effect on the brainstem oxidative stress indicating that any vagal insult is presumably peripheral in nature. Moreover, rivaroxaban treatment revealed that CAN can be ameliorated by direct effects on the cardiovascular system and AT releasing factor Xa, or indirectly by affecting macrophages expressing PARs.

In conclusion, rivaroxaban showed promising results in interrupting thrombo-inflammation and ameliorating adipose tissue inflammation which eventually might have improved the baroreceptor sensitivity and mitigated CAN.

# TABLE OF CONTENTS

ACKNOWLEDGEMENTS .....	1
ABSTRACT .....	2
ILLUSTRATIONS .....	6
ABBREVIATIONS .....	7
I. INTRODUCTION.....	10
A. Diabetes: Definition, Classification, and Epidemiology: .....	10
B. Prediabetes: .....	10
C. Prediabetes and Adipose Tissue Inflammation: .....	12
1. General Overview of Adipose Tissue and Perivascular Adipose Tissue Inflammation.....	12
2. PVAT Inflammation and Thrombo-inflammation.....	15
D. Cardiac Autonomic Neuropathy (CAN): .....	15
1. History of CAN and its Prognosis .....	15
2. CAN Diagnosis and Parameters .....	17
3. Clinical Manifestations of CAN .....	18
4. CAN and Adipose Tissue Inflammation.....	19
E. Pharmacological Treatment for CAN: .....	21
1. Direct Oral Anticoagulants (DOACs) Overview .....	21
2. Rivaroxaban: Mechanism of Action .....	22
3. Rivaroxaban and Inflammation .....	23
F. Rationale, Hypothesis, and Aims: .....	23

II. MATERIALS AND METHODS .....	24
A. Ethical Approval: .....	24
B. Experimental Design: .....	24
C. Food Preparation and Micronutrient Composition: .....	25
D. Regular Gross Examination, Blood Tests, Sacrifice, and Organs Harvest: .....	25
E. Measurement of Hemodynamic Function: .....	26
F. Baroreceptor Sensitivity (BRS): .....	26
G. Nuclear Magnetic Resonance (NMR): .....	27
H. Blood Chemistry: .....	27
I. Immunofluorescence and Histopathology Studies: .....	27
J. Western Blotting: .....	28
K. Statistical Analysis: .....	29
L. Chemicals: .....	29
III. RESULTS .....	30
A. Metabolic Consequences of HC Feeding: .....	30
B. Baroreceptor Sensitivity with Single Treatments: .....	31
1. Cardiac (HR) and Vascular (MAP) Responses to Vasopressor, Phenylephrine 31	
2. Cardiac (HR) and Vascular (MAP) Responses to Vasodilator, Sodium Nitroprusside .....	34
C. Impact of Rivaroxaban Treatment on PVAT Inflammation in HC-Fed Rats: ....	37
D. Impact of Rivaroxaban Treatment on PVAT Adipocyte Hypertrophy and Oxidative Stress in HC-Fed Rats: .....	37

E. Impact of Rivaroxaban Treatment on Brainstem Oxidative Stress in HC-Fed Rats: .....	39
F. Microscopic, Oxidative, and Inflammatory Changes in Ventricular Tissues:.....	40
1. Hematoxylin and Eosin (H&E) Staining: .....	40
2. Masson Trichrome Staining:.....	40
3. Dihydroethidium (DHE) Staining:.....	40
 IV. DISCUSSION .....	 42
 V. LIMITATIONS AND FUTURE DIRECTIONS .....	 46
 REFERENCES .....	 47



## ILLUSTRATIONS

### Figure

1. Excessive Caloric Intake Effect on the Adipose Tissue .....	14
2. Daily Caloric Intake and Metabolic Parameters of Rats in Different Treatment Groups.....	30
3. The Effect of HC Feeding and Treatment with Rivaroxaban on the Sensitivity of the Parasympathetic Arm of the Baroreflex .....	32
4. Representative Tracings of Pressor [Mean Arterial Pressure (MAP)] and Cardiac [Heart Rate (HR)] Responses to Increasing Doses of Vasopressor Phenylephrine (PE) in Normal Controls, HC-Fed Rats, and Rivaroxaban Treated Rats .....	33
5. The Effect of HC Feeding and Treatment with Rivaroxaban on the Sensitivity of the Sympathetic Arm of the Baroreflex .....	35
6. Representative Tracings of Depressor [Mean Arterial Pressure (MAP)] and cardiac [Heart Rate (HR)] Responses to Increasing Doses of Vasodilator Sodium Nitroprusside (SNP) in Normal Controls, HC-Fed Rats, and Rivaroxaban Treated Rats .....	36
7. The Effect of HC Feeding and Treatment with Rivaroxaban on Inflammatory Cytokine Expression in Perivascular Adipose Tissue .....	37
8. The Effect of Mild Hypercaloric Diet and Rivaroxaban Treatment on Perivascular Size and Oxidative Stress.....	38
9. The Effect of Mild Hypercaloric Diet and Rivaroxaban Treatment on Brainstem Oxidative Stress .....	39
10. Structural and Molecular Changes in Ventricular Tissue in Response to HC Feeding and Rivaroxaban Treatment .....	41

## ABBREVIATIONS

CAN: Cardiac Autonomic Neuropathy

T2D: Type 2 Diabetes

AT: Adipose Tissue

WAT: White Adipose Tissue

BAT: Brown Adipose Tissue

BeAT: Beige Adipose Tissue

PVAT: Perivascular Adipose Tissue

DOACs: Direct Oral Anticoagulants

OACs: Oral Anticoagulants

NMR: Nuclear Magnetic Resonance

HC: High Calorie

HR: Heart Rate

MAP: Mean Arterial Pressure

ADA: American Diabetes Association

IFG: Impaired Fasting Glucose

FPG: Fasting Plasma Glucose

OGTT: Oral Glucose Tolerance Test

HRV: Heart Rate Variability

BRS: Baroreceptor Sensitivity

TNF- $\alpha$ : Tumor Necrosis Factor alpha

NO: Nitric Oxide

ROS: Reactive Oxygen Species

UCP-1: Uncoupling Protein 1

IL-1 $\beta$ : Interleukin-1 $\beta$

IL-6: Interleukin-6

HIF-1 $\alpha$ : Hypoxia Inducible Factor-1 alpha

IKK $\beta$ : Inflammation-induced I $\kappa$ B kinase – $\beta$

NF- $\kappa$ B: Nuclear Factor Kappa B

PARs: Protease-Activated Receptors

ACCORD: Action to Control Cardiovascular Risk in Diabetes

PSNS: Parasympathetic Nervous System

SNS: Sympathetic Nervous System

CNS: Central Nervous System

BP: Blood Pressure

HF: High Frequency

LF: Low Frequency

PE: Phenylephrine

SNP: Sodium Nitroprusside

CO: Cardiac Output

SBP: Systolic Blood Pressure

DBP: Diastolic Blood Pressure

IACUC: Institutional Animal Care and Use Committee

CTRL: Control

MHC: Mild hypercaloric

RIVA: Rivaroxaban

DHE: Dihydroethidium

SDS: Sodium Dodecyl Sulfate

BBB: Blood Brain Barrier

VSMCs: Vascular Smooth Muscles Cells

ECs: Endothelial Cells

# CHAPTER I

## INTRODUCTION

### **A. Diabetes: Definition, Classification, and Epidemiology:**

Diabetes is a worldwide epidemic with a huge economic burden. In 2019, it was estimated that about 463 million adults worldwide lived with diabetes, especially in the low- and middle-income countries. This number is predicted to increase by 2045 reaching 700 million adults with 1.5 million diabetes related deaths annually (1-3).

Diabetes mellitus is a chronic metabolic disorder characterized by elevated levels of blood glucose and includes two types. Type 1 is a consequence of the autoimmune destruction of the beta cells of the pancreas causing the lack of insulin, while type 2 which is more prevalent, is related to insulin resistance and insulin deficiency (4, 5).

Diabetes is associated with long-term macrovascular and microvascular complications. The former are mainly represented by endothelial dysfunction, atherosclerosis, and arterial stiffening leading to cerebral and peripheral vascular diseases. As for the latter, diabetic patients are prone to develop retinopathy, nephropathy, and neuropathy (6).

### **B. Prediabetes:**

Prediabetes precedes type 2 diabetes mellitus (T2D), and is characterized by glycemic levels that do not meet the diabetes diagnostic criteria; however they are too high to be considered normal (7). During this stage insulin resistance appears as an impaired response of peripheral tissues, such as adipose tissues, muscles, and the liver, to the normal insulin concentrations. As a consequence, hyperinsulinemia kicks in as a

compensatory mechanism for reduced insulin sensitivity. Later, exhaustion of the beta cells results in insulin deficiency triggering hyperglycemia (8, 9).

The blood glucose level remains normal in the early stages because of the release of large amounts of insulin trying to compensate for insulin resistance, causing the pancreatic beta-cells' mass to increase. Later in time, the beta-cells cannot keep up, and insulin resistance aggravates thus leading to sustained hyperglycemia and type 2 diabetes mellitus down the road (10). Significantly, the American Diabetes Association (ADA) estimates that about 70% of individuals with prediabetes will progress to diabetes later in time (11).

Prediabetes is mainly characterized by impaired fasting glucose (IFG) reflected by abnormal fasting plasma glucose (FPG) levels, and/or impaired glucose tolerance (IGT) detected based on a 2-h oral glucose tolerance test (OGTT) measured after the ingestion of 75g of glucose solution. Additionally, ADA introduced the HbA1C as a measure of the levels of glycated hemoglobin, as a diagnostic marker of prediabetes (11). Particularly, prediabetes is diagnosed by the presence of at least one of the following criteria, FPG level of 100 to 125 mg/dL, OGTT level of 140 to 199 mg/dL, and/or HbA1c level of 5.7 to 6.4% (9).

A study done by Sorensen et al. (the Maastricht Study) revealed that patients newly diagnosed with diabetes suffer from established cardiovascular complications linking their pathogenesis to prediabetes (12). Indeed, prediabetes is associated with an increased risk of both premature microvascular and macrovascular diseases (13). Cardiac autonomic neuropathy is one of the early microvascular complications evident in prediabetes that is characterized by parasympathetic dysfunction assessed by heart rate variability (HRV) and baroreceptor sensitivity (BRS) (7, 11).

## **C. Prediabetes and Adipose Tissue Inflammation:**

### ***1. General Overview of Adipose Tissue and Perivascular Adipose Tissue***

#### ***Inflammation***

Adipose tissues (AT) consist of lipid-rich cells called adipocytes, and are found in different compartments of the human body, namely, parietal or subcutaneous (embedded in the connective tissue), and visceral (surrounding internal organs) (14). In addition to the adipocytes, connective tissue matrix, stroma-vascular cells, nerve tissue, and immune cells are found in ATs (15, 16). ATs were originally viewed as simple storage sites for triacylglycerol and energy, but are now regarded as complex and highly active metabolic and endocrine organs (15, 16).

In mammals, adipose tissues are divided into two classical and functional adipocytes, white and brown. White adipose tissue (WAT) is formed of unilocular adipocytes comprising dual actions; the first being a storage site for lipids and fats with the ability to release fatty acids when fuel is needed; the second is secreting a number of biologically active molecules known as adipokines (leptin, adiponectin,...), cytokines/chemokines (interleukin 6 “IL-6”, tumor necrosis factor alpha “TNF- $\alpha$ ”, ...), gaseous molecules (nitric oxide “NO”,...), prostacyclin, angiotensin-1 to 7, and reactive oxygen species “ROS” (17). On the contrary, brown adipose tissue (BAT) is formed of multilocular adipocytes expressing numerous mitochondria exhibiting the uncoupling protein 1 (UCP-1), a proton transporter upregulated by  $\beta$ 3 adrenoceptors stimulation. Moreover, BAT is a highly vascularized pool, responsible for the non-shivering thermogenesis mediated by UCP-1 through uncoupled respiration thus consuming oxygen to expend energy (14, 16, 18). Recently, discoveries revealed the presence of brown-like adipocytes dispersed within the white adipocytes; this mixture was referred

to as “Beige” adipose tissue “BeAT”. BeAT possesses UCP-1 in low amounts, however, once stimulated, the expression of UCP-1 increases to a level similar to that of BAT (14, 16, 18). As such, the beige cells alternate between an energy storage and energy dissipation phenotype (19).

Importantly, visceral WAT comprises epicardial, retroperitoneal, mesenteric, perirenal, and perivascular adipose tissue (20). Perivascular adipose tissue (PVAT) is a pool surrounding the blood vessels and was recognized as a connective tissue supporting the vessel at first; later on, it demonstrated important effects on the vascular function and homeostasis (17, 21). PVAT are formed mainly of “Beige” adipocytes (17) with resident immune cells capable of releasing pro-inflammatory cytokines, such as TNF-  $\alpha$ , IL-6, and interleukin-1 $\beta$  (IL-1 $\beta$ ) in the setting of a disease shifting the microenvironment into an inflammatory one (22, 23). In addition, adipocytokines are also being released, such as adiponectin, a protective adipokine responsible for suppressing ROS generation and reducing pro-inflammatory factors release, and leptin, a pro-inflammatory cytokine playing a role in energy homeostasis and ROS generation (16, 17).

In cases of obesity or chronic increase in calorie consumption, perivascular adipocytes expand in an attempt to accommodate excess calories further leading to insulin resistance (24). As such, the poorly vascularized environment manifested by hypertrophy culminates in hypoxia and activation of hypoxia inducible factor-1 alpha (HIF-1 $\alpha$ ) promoting oxidative stress and the release of pro-inflammatory cytokines and adipokines (24). Hypoxia will also cause lipotoxicity culminating in adipocyte apoptosis and cell death, leading to macrophages recruitment in an attempt to resolve and repair the damaged tissue (25, 26). At the same time, AT inflammation is further



exacerbated by the following mechanism. An increase in the sympathetic outflow further stimulating  $\beta_3$  adrenergic receptors allowing the upregulation of UCP-1 further aggravating the hypoxic milieu, and the stimulation of inflammation-induced I $\kappa$ B kinase  $-\beta$  (IKK $\beta$ ) pathway accelerating the activation of the transcription factor nuclear factor-kappa B (NF- $\kappa$ B) (24) (Fig.1). Subsequently, a study done by ElKhatib et al. (2019) revealed that prediabetic high fat diet fed-rats manifested localized PVAT inflammation associated with vascular dysfunction prior to the development of overt hyperglycemia (24).

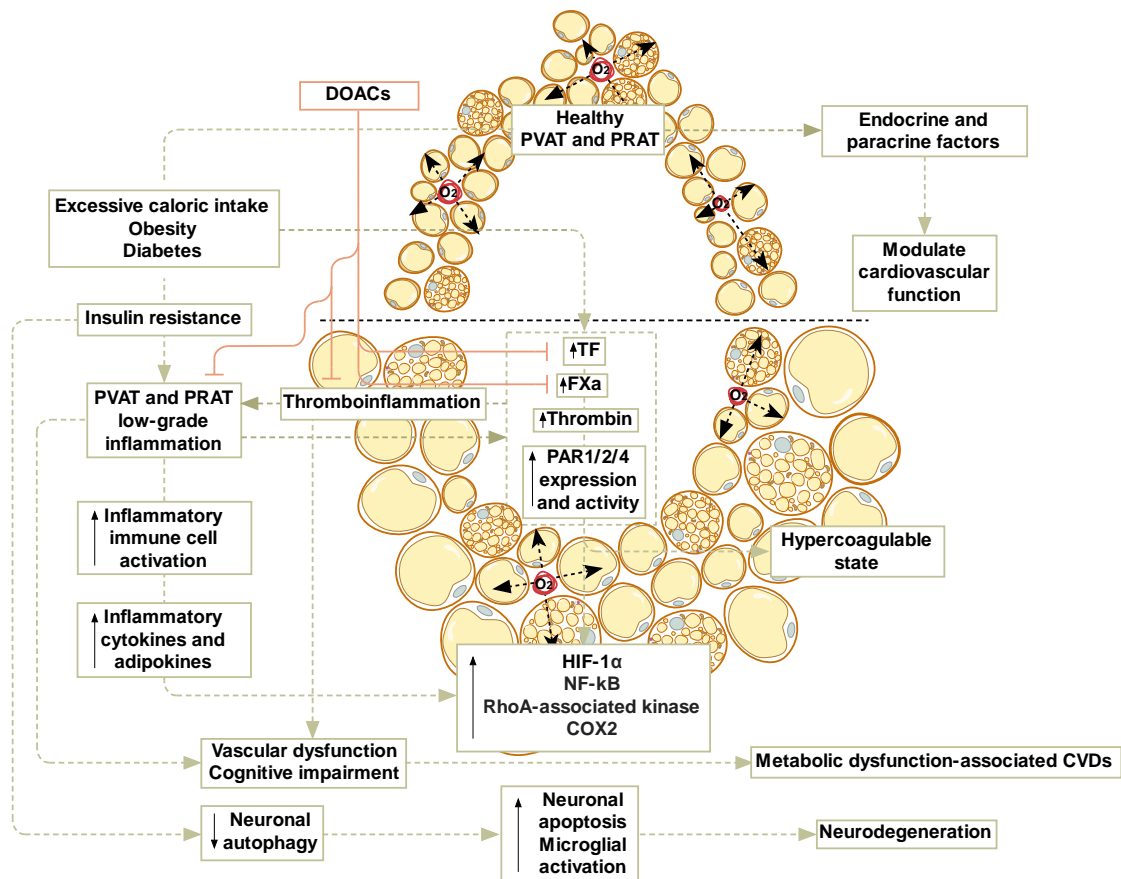


Figure 1: Excessive caloric intake effect on the adipose tissue (27).

## ***2. PVAT Inflammation and Thrombo-inflammation***

When blood vessels become injured, repair requires the presence of two major components, the coagulation factors and blood platelets, responsible for initiating the clotting cascade (28). Consequently, two major pathways will be activated, the extrinsic and intrinsic pathways (29). Inflamed adipose tissue specifically will produce a huge amount of tissue factor activating this clotting cascade and resulting in elevated levels of thrombin and factor Xa (24). Activated factor Xa later will cleave prothrombin into thrombin, which will cleave fibrinogen into fibrin forming a clot to seal the injury (29). Interestingly, activated factor Xa and thrombin act on several tissues expressing protease-activated receptors (PARs) such as adipocytes leading to adipose tissue inflammation (29).

Alternatively, in a vicious cycle, adipose tissue inflammation elevates the expression of tissue factor which in turn activates the clotting cascade. The subsequent increase in factor Xa and thrombin levels will activate protease-activated receptors (PARs) 1 and 2 triggering thromboinflammation (30, 31). Such a condition is associated with visceral adipose tissue inflammation leading to deposition of macrophages releasing tumor necrosis factor  $\alpha$  and interleukins (IL) 1 $\beta$  and 6 that will reduce insulin sensitivity of adipocytes (32). Factor Xa activates both PARs 1 and 2, while thrombin activates PAR 1 only.

### **D. Cardiac Autonomic Neuropathy (CAN):**

#### ***1. History of CAN and its Prognosis***

Cardiac autonomic neuropathy (CAN) is defined as a dysfunction in the autonomic nerve fibers innervating the heart and blood vessels resulting in

abnormalities in the heart rate and vascular tone (33). It is one of the earliest underdiagnosed manifestation of types 1 and 2 diabetes; around 25.3% of type 1 diabetic patients and 34.3% of type 2 diabetic patients suffer from CAN (34). In fact, presence of CAN predisposes for the development of cardiovascular dysfunction which usually progresses into myocardial ischemia, stroke, coronary artery disease, and overall morbidity and mortality (35). Indeed, results from the Action to Control Cardiovascular Risk in Diabetes (ACCORD) study indicate that mortality rate in diabetic patients is 1.55-2.14 times greater than those without diabetes (36). Importantly, it is recommended by the Toronto Consensus Panel on Diabetic Neuropathy that patients on their first diagnosis with type 2 diabetes get screened for CAN. This is based on evidence showing that CAN development is independent of hyperglycemia, but rather related to metabolic disorders and dyslipidemia (33), hallmarks of prediabetes (37).

Diabetes can induce CAN either directly through neuronal dysfunction, or indirectly through cardiovascular dysfunction such as dilated cardiomyopathy and aortic stiffness, precipitating insults to autonomic control (37). In fact, CAN is a progressive disorder. During its early stages, a deterioration in vagus nerve (longest autonomic nerve) function brings about a reduction in parasympathetic activity and a subsequent predominance of the sympathetic tone. The latter is known as the sub-clinical stage, and is detected by abnormalities in the frequency and time domains of the spectral analysis of heart rate variability (HRV) and baroreflex sensitivity (BRS) tests. CAN will further lead to reduced sympathetic activity in advanced stages, manifested as postural hypotension (38). It is estimated that many sub-clinical CAN patients will progress into clinical CAN within 5 years (38, 39).

## ***2. CAN Diagnosis and Parameters***

The autonomic nervous system is divided into two arms comprising the parasympathetic and the sympathetic nervous systems (PSNS and SNS, respectively) (40). The first is responsible for decreasing the heart rate (HR) and increasing the heart rate variability (HRV), while the other handles the opposite functions (41).

Baroreceptors present in the carotid artery and aortic arch are pivotal in controlling and adjusting the blood pressure (BP) and heart rate (HR) (42). Particularly, changes in arterial blood pressure are sensed by the baroreceptors as increases or decreases in their stretch. Input from baroreceptors is relayed to the medulla (the integrative center) through afferent nerves, then the output is transmitted by an efferent pathway to the effector organ (heart or vascular beds) (42, 43). Additionally, cardiac autonomic function is largely dependent on the integrity of the previously mentioned reflex arc: baroreceptor – afferent nerve – brainstem – efferent nerve – effector organ (42).

HRV is a diagnostic technique for CAN (44). In fact, this variability stems from the two opposing systems: parasympathetic which slows the firing of the sinoatrial node and the sympathetic which accelerates it (45). HRV is categorized by linear and non-linear indices. The former includes time domain parameter (diagnostic of the parasympathetic function) and frequency domain parameter (consisting of high frequency (HF) representative of parasympathetic activity, and the low frequency (LF) indicative of the sympathetic activity) (33). While, the latter parameters are analyzed from Poincare plot of R-R intervals (45).

BRS measures the change in HR in response to changes in BP (46). The most common tools to assess BRS are the Valsalva maneuver, the vasoactive drug procedure, and the neck chamber method. Regarding Valsalva maneuver, it challenges the

baroreceptors by abrupt elevations in intrathoracic and intraabdominal pressures through straining. This method is achieved by performing forced expiration against a closed airway, and the patient should be lying in a supine position while the ECG and beat-to-beat arterial pressure are being recorded (46). As for the vasoactive method, increasing doses of phenylephrine (PE) are administered to assess the parasympathetic function. PE is an alpha-adrenergic agonist that only raises the BP without directly affecting the HR or the central nervous system (CNS). Changes in BP along with their reflex bradycardic responses are recorded for every PE dose. Values are then fitted into a linear regression line, the slope of which is representative of parasympathetic BRS (46, 47). On the other hand, a vasodepressor agent called sodium nitroprusside (SNP) is used to examine the sympathetic activity (33, 46). Concerning the neck chamber method, it involves a mechanical activation or deactivation of the carotid baroreceptors by applying positive or negative pressure of known values to the neck region. An increase in the neck chamber pressure is sensed as a decrease in arterial pressure evoking a reflex response through vagal withdrawal and sympathetic stimulation to the heart and vessel beds thus increasing the blood pressure and heart rate (46).

### ***3. Clinical Manifestations of CAN***

As discussed earlier, several studies have found that patients on their first diagnosis with diabetes are already suffering from established cardiovascular complications confirming the existence of prediabetes (13, 48). Specifically, CAN is one of the early cardiovascular complications present in newly-diagnosed patients before the advent of overt hyperglycemia. Subsequently, clinical symptoms appear progressively with the development and progress of decompensated insulin resistance

(38). At the early stages of the disease, the “sub-clinical stage”, resting tachycardia and exercise intolerance take place as a result of parasympathetic neuronal damage and subsequent sympathetic augmentation. This is manifested as an increase in the heart rate reaching 90 – 130 beats per minute. This sympathovagal imbalance alters the BP, HR, and cardiac output (CO) in the absence of structural or coronary cardiac disease (33, 38). As the disease progresses, the sympathetic activity becomes blunted leading to orthostatic hypotension secondary to vasoconstriction and blunted BRS impairing HR responses. This is manifested by a fall in both the systolic blood pressure (SBP) and diastolic blood pressure (DBP) of more than 20 mmHg and 10 mmHg, respectively, in response to a postural change (33, 38). Furthermore, intraoperative and perioperative cardiac instability is also a clinical manifestation of CAN, whereby the patients require vasopressor support during the induction of general anesthesia, due to the severe BP and HR reductions that they may experience (38, 49).

#### ***4. CAN and Adipose Tissue Inflammation***

Upon fat accumulation and hypertrophy, the visceral adipose tissue, releases a variety of proinflammatory cytokines/adipokines, such as TNF- $\alpha$  and IL-6, leading to hyperinsulinemia and insulin resistance (50). Hyperinsulinemia disrupts the autonomic balance and cause sympathetic dominance (48). A study done by Lieb et al. (2012) revealed that a correlation exists between autonomic function and inflammatory markers; where an autonomic imbalance can be associated with inflammatory changes in adipose tissue, which presents that an increase in the levels of IL-6 along with abnormal parasympathetic and sympathetic function in newly diagnosed and established diabetic patients (50). Interestingly, Thiagarajan et al. (2012) showed that patients with

impaired fasting glucose (IFG) had elevated levels of TNF- $\alpha$ , pointing out to the existence of a subclinical inflammatory state in prediabetes (51). Importantly, this is accompanied with an increase in the HR and altered cardiac autonomic function; LF/HF ratio was shown to be higher in the IFG group revealing early parasympathetic dysfunction. Furthermore, markers of oxidative stress in the vasculature were shown to be related to this autonomic dysregulation, i.e. parasympathetic blunting (51).

Additionally, adiponectin loses its anti-inflammatory properties in the obese diabetic patients. Consequently, a decrease in serum adiponectin was linked to a sympathetic overdrive (demonstrated by an increase in the LF/HF ratio of HRV spectral analysis) leading to cardiovascular disorders development and insulin resistance (52).

Accordingly, two directions for the relationship between CAN and adipose tissue inflammation commence; the first implicates adipose tissue inflammation as a risk factor for CAN development through the several inflammatory markers being released, thus deteriorating the cardiovascular and neural function; whereas the other presents exaggerated adipose inflammation as a consequence of autonomic deterioration. In fact, the blunted parasympathetic system manifested by the loss of vagus nerve's function exacerbates inflammation. Thus, the vagal nerve is important in regulating and preventing tissue damage from exaggerated inflammatory responses by reducing the production of TNF- $\alpha$  and the migration of leukocytes to the site of inflammation (53).

## **E. Pharmacological Treatment for CAN:**

During the late stages of CAN, it becomes symptomatic and irreversible. Therefore, it is essential to look for pharmacological treatments that can delay the progression of CAN into life-threatening complications (54). A previous study in our laboratory revealed an association of early CAN with perivascular adipose tissue inflammation during an early stage of metabolic challenge with a mild hypercaloric diet (55). Indeed, treatment with anti-diabetic agents with known anti-inflammatory effects, such as metformin, was successful in reversing PVAT inflammation and its detrimental consequences, such as CAN, through targeting adipose tissue inflammation. Consequently, in an attempt to further elucidate the pro-inflammatory mechanisms responsible for CAN pathogenesis, we used a direct oral anticoagulant to target thromboinflammation involved in the deleterious process.

### ***1. Direct Oral Anticoagulants (DOACs) Overview***

Oral anticoagulants (OACs) belong to a group of drugs used to treat thrombosis secondary to the activation of factor Xa and thrombin, with the subsequent conversion of soluble fibrinogen to insoluble fibrin (clot forming unit) and activation of platelets. Additionally, exaggerated secretion of pro-inflammatory mediators and coagulation factors arising during injury, leads to perivascular and thromboinflammation, thus giving rise to neuronal and vascular dysfunction during prediabetes (27).

Direct oral anticoagulants (DOACs) are small molecules proven to be safe, stable, easily dispersed throughout the body, and it have a rapid onset of action (56-58). DOACs were approved to be used for stroke prevention, treatment of deep vein



thrombosis, and pulmonary embolism by dissolving clots and preventing their propagation through fibrinolysis and inhibition of procoagulation factors (59).

DOACs are classified into two categories: thrombin and factor Xa inhibitors. Thrombin inhibitors, such as dabigatran, bind directly to thrombin and prevent it from cleaving fibrinogen to fibrin. On the other hand, factor Xa inhibitors, such as rivaroxaban, bind directly to Factor Xa, inhibiting the cleavage of prothrombin to thrombin. Thrombin and factor Xa inhibitors are common to both the intrinsic and extrinsic activation pathways, and capable of inhibiting the activation of PAR 1 and 2 (59). Owing to their capacity to attenuate PARs expression, tissue fibrosis, inflammation, and ROS production, DOACs were shown to be able to interrupt the thromboinflammatory loop (27).

## ***2. Rivaroxaban: Mechanism of Action***

Rivaroxaban is a reversible, selective direct inhibitor of factor Xa (60). It does not only inhibit the conversion of prothrombin to thrombin, but also factor Xa-mediated activation of PAR 1 and 2 on tissues. Thus, it can act as a potent anti-inflammatory drug by mainly alleviating PAR-2-mediated inhibition of macrophage autophagy, reducing the release of pro-inflammatory cytokines and increasing eNOS activity (27, 61). It was also proven by Hashikata et al. that rivaroxaban can reduce cellular migration, proliferation, and production of inflammatory cytokines by inhibiting NF-kB and MAPK/AP-1 pro-inflammatory signaling pathways (27, 62). Hence, factor Xa inhibition by rivaroxaban not only reduces the risk of death, myocardial infarction, and stroke, but also restores vascular function and reduces inflammation (63).

### **3. Rivaroxaban and Inflammation**

Localized perivascular adipose tissue inflammation resulting from metabolic challenges, is associated with vascular contractile abnormalities and cardiac autonomic neuropathy (24). Thromboinflammation resulting from increased levels of factor Xa and PAR 1, 2 expressions and activities, leads to vascular injury and atherosclerosis thus aggravating adipose tissue inflammation (27). Rivaroxaban treatment ameliorates adipose tissue inflammation alleviating insulin resistance, and improves the overall metabolic profile (64).

#### **F. Rationale, Hypothesis, and Aims:**

Our laboratory has shown that CAN can be ameliorated using medications proven to have anti-inflammatory actions. Additionally, previous studies showed that metabolic challenge in prediabetes is accompanied with elevated factor Xa levels as well as PAR 1 and 2 expression and activity. Hence, we hypothesize that interrupting thromboinflammation by inhibiting factor Xa and PAR 1 / 2 activities reduces the burden of perivascular adipose tissue inflammation and ameliorates CAN.

Thus, we aimed to:

- 1- Study changes in cardiac autonomic function detected by baroreflex sensitivity in control, MHC-fed rats, and those treated with rivaroxaban.
- 2- Assess the status of perivascular adipose tissue inflammation in control, MHC-fed rats, and those treated with rivaroxaban.
- 3- Assess the status of the brainstem and cardiac tissues in control, MHC-fed rats, and those treated with rivaroxaban.

## CHAPTER II

### MATERIALS AND METHODS

#### **A. Ethical Approval:**

All animal experiments were done in accordance with study protocol number 16-10-386 approved by AUB Institutional Animal Care and Use Committee (IACUC) in compliance with the Guide for the Care and Use of Laboratory Animals of the Institute for Laboratory Animal Research of the National Academy of Sciences, U.S.A.

#### **B. Experimental Design:**

Male Sprague-Dawley rats (5-6 weeks of age; 150g) were randomly allocated to three different groups (n=8 each): (1) a control group comprising rats on normal chow diet (3 Kcal/g, CTRL) for 12 weeks, (2) an experimental group comprising rats on mild hyper caloric diet (4.035 Kcal/g) (MHC rats) for 12 weeks, (3) an experimental group comprising rats on mild hyper caloric diet (4.035 Kcal/g) for 12 weeks during which rivaroxaban (20mg/kg) treatment (RIVA rats) was implemented at week 10 and continued for the remaining two weeks. Additionally, both MHC and RIVA experimental rats were provided with 20% fructose water for 2 weeks starting week 10, to promote hyperinsulinemia and manifest a massive adipose tissue inflammation. All rats had free access to food and water for the full 12-week duration. Rats were kept in a temperature- and humidity- controlled room, in a 12-hour light/dark cycle. Body weight was measured weekly and calorie intake was calculated based on the amount of food consumed. The treatment was freshly prepared on daily basis by adding the required amount out of the 20 mg of rivaroxaban powder to a 5g wet-chow pellet of the high fat

diet, then the drug-containing food pellet was administered to the RIVA group for 2 weeks starting week 10 daily.

### **C. Food Preparation and Micronutrient Composition:**

Normal chow diet (ENVIGO) was obtained from Teklad Rodent Diets (Madison, WI). This diet offers 3 Kcal/g distributed as follows: 32% from protein, 14% from fat (of which 0.9% by weight saturated fat), and 54% from carbohydrates. The MHC diet was prepared in house through the addition of food grade fructose (20% by weight, Santiveri Foods, Spain) and hydrogenated vegetable oil (Mazola®, 15% by weight, BFS). Major electrolytes and vitamins were supplemented to match the concentration in ENVIGO diet. The final composition by weight of the MHC diet (calorie content) is: 18.06% fat (38.68%, 5% saturated fat by weight), 15.8% protein (15.66%), and 46.13% carbohydrates (45.73%). All diets were fed for a period of 12 weeks.

### **D. Regular Gross Examination, Blood Tests, Sacrifice, and Organs Harvest:**

At the end of week 12, the rats were anesthetized by 50 mg/mL thiopental, and the hemodynamic study was performed. At the end, the rats were decapitated and blood was collected. The head was placed in ice and the brainstem was isolated. The thoracic cavity was exposed and the heart was flushed and isolated. The atria were removed and the ventricles were weighed and horizontally cut into three sections (apex, mid-section, and base). The mid-section was placed in formaldehyde for further histological analysis. Other tissues were stored at -80°C. The tibia bone length was measure for normalization purposes.

### **E. Measurement of Hemodynamic Function:**

The hemodynamic study was performed at week 12. Rats were anesthetized using 50 mg/mL of thiopental for induction. Tracheostomy was performed and right carotid artery was isolated, cannulated and connected to a Millar transducer to measure mean arterial pressure (MAP) and heart rate (HR). After this, the left jugular vein was isolated, cannulated, and connected to a shunt to deliver drugs. After surgery was done, the recording was allowed to stabilize for 30 minutes. Increasing doses of Phenylephrine (PE) were given (0.25, 0.5, 0.75, 1, and 2  $\mu\text{g}$ ) and the changes in MAP and HR were recorded. After giving the vasoconstrictor, the rat is allowed to rest for another 30 minutes after which ascending doses of Sodium Nitroprusside (SNP) were administered (0.75, 1, 2, 4, and 8  $\mu\text{g}$ ). Again, the changes in MAP and HR in response to SNP were recorded.

### **F. Baroreceptor Sensitivity (BRS):**

The vasoactive method was used to assess BRS. It was determined using modified Oxford method, where the relationship between cardiac autonomic control, and mean arterial pressure during different vasoactive drug dose administration was calculated. The slope of the linear regression fit between  $\Delta\text{MAP}$  and  $\Delta\text{HR}$  was determined and used to validate the functionality of the baroreceptors. And so the steeper the slope, the better is the sensitivity and thus the functionality of the baroreceptors.

### **G. Nuclear Magnetic Resonance (NMR):**

The body composition of the rat (lipids, proteins, water) was analyzed using the nuclear magnetic resonance machine (LF10 Minispec NF4433, Bruker, MA, USA). The animal was weighed and placed inside a cylindrical plastic box where it was made immobile by squeezing it against the lower bottom of the cylinder. After which the cylinder containing the rat was inserted inside the NMR machine and the following parameters were estimated: fat mass, lean mass, fluid content, and the fat/lean ratio to detect different tissue densities. The body composition measurement was performed at a 4-week interval and values obtained from each rat were compared to a standardized, calibrated rat.

### **H. Blood Chemistry:**

Total serum triglyceride was assessed in all groups. Blood samples (0.7 ml) were taken by retro-orbital bleeding and centrifuged at 4000 rpm for 10 minutes. The supernatant serum was isolated and stored at 280°C till the time of analysis. Total serum triglyceride was measured using electrochemiluminescence on a Cobas 6000 reader (Roche Diagnostics, Basel, Switzerland).

### **I. Immunofluorescence and Histopathology Studies:**

The heart mid-sections placed in 10% formaldehyde solution were fixed in 100% ethanol, embedded in paraffin, cut transversely, and placed on slides. The staining was done simultaneously to all the slides for accurate comparison. Hematoxylin and Eosin (H&E) staining was used for the demonstration of nucleus and cytoplasmic inclusion, while Masson Trichrome was performed to detect cardiac fibrosis.

Dihydroethidium (DHE) staining was further used to detect reactive oxygen species presence in the heart, thoracic PVAT, and brainstem.

#### **J. Western Blotting:**

Protein extraction and western blotting were carried out using a technique formerly developed and optimized in our laboratory. In summary, thoracic PVAT samples stored at -80°C were crushed under liquid nitrogen. Tissues were transferred to protein extraction buffer containing 1% sodium dodecyl sulfate (SDS), 0.9% NaCl, 80 mM Tris hydrochloride (pH 6.8), and 100 mM dithiothreitol. Tissue amount used for protein extraction were optimized with respect to final protein concentrations in preliminary experiments. Samples were heated for 10 minutes at 95°C, allowed to cool down and transferred to a rocking shaker and left overnight for protein extraction at 4°C. Aliquots with equal protein content from the extracts were then used for SDS-PAGE and blotting as described previously. After transfer and fixation, nitrocellulose membranes were blocked with 5% skim milk (Bio-Rad, Hercules, CA, USA) in Tris-buffered saline containing 0.1% Tween 20 for two hours at room temperature. At this stage, membranes were cut at the appropriate molecular weights to allow for probing of multiple proteins within the same run. Membranes were incubated in a dilution of primary antibodies in 0.1% TBST (1:500 for rabbit polyclonal anti-IL-1 $\beta$ ) overnight at 4°C. After washing with 0.05% TBST (4x5 mins), membranes were incubated in 1:10,000 biotin-conjugated goat anti-rabbit Ig for 1 hour at room temperature followed by washing and incubation with 1:100,000 horse-radish peroxidase-conjugated streptavidin at room temperature for 30 minutes. Following washing 4x5 min with 0.05% TBST and 2x5 min with TBS, membranes were exposed to Clarity Western ECL

substrate (BioRad, Hercules, CA) for 5 min followed by image detection using ChemiDoc imaging system (BioRad, Hercules, CA). Band optical density was measured using Image J software and a ratio of arbitrary density units was obtained for the protein band of interest. IL-1 $\beta$  was normalized to actin as described previously to correct for variabilities in loading and sample concentration.

#### **K. Statistical Analysis:**

Data were expressed by Mean  $\pm$  SEM. All analysis was done using PRISM software. Comparisons between the different groups were done using One-way ANOVA followed by Tukey's *post-hoc* test, Two-way ANOVA followed by Sidak's multiple comparisons test (to compare different time points or doses among groups), or Student's *t*-test as appropriate using GraphPad Prism Software. A *P*-value < 0.05 was considered statistically significant.

#### **L. Chemicals:**

All chemicals were obtained from Sigma (St. Louis, MO) unless otherwise indicated. Pharmaceutical grade Rivaroxaban was a kind gift from regional manufacturers (Pharo Pharma and Hikma Pharmaceuticals).



## CHAPTER III

### RESULTS

#### A. Metabolic Consequences of HC Feeding:

During the experimental period, HC-fed rats, with or without rivaroxaban treatment, significantly consumed more calories compared to the control rats (Fig. 2A). Moreover, at week 10, a significant rise was manifested after the introduction of fructose water to these two groups. All rats started with approximately the same weight (150 g), and continued to gain weight in the same manner despite the increased caloric intake (Fig. 2B). However, an increase in the fat to lean ratio was observed in both the HC-fed rats and the rivaroxaban treated rats indicating adipose expansion (Fig.2C). Serum triglyceride level was significantly higher in both the HC-fed rats and rivaroxaban treated rats confirming the presence of a metabolic insult (Fig.2D).

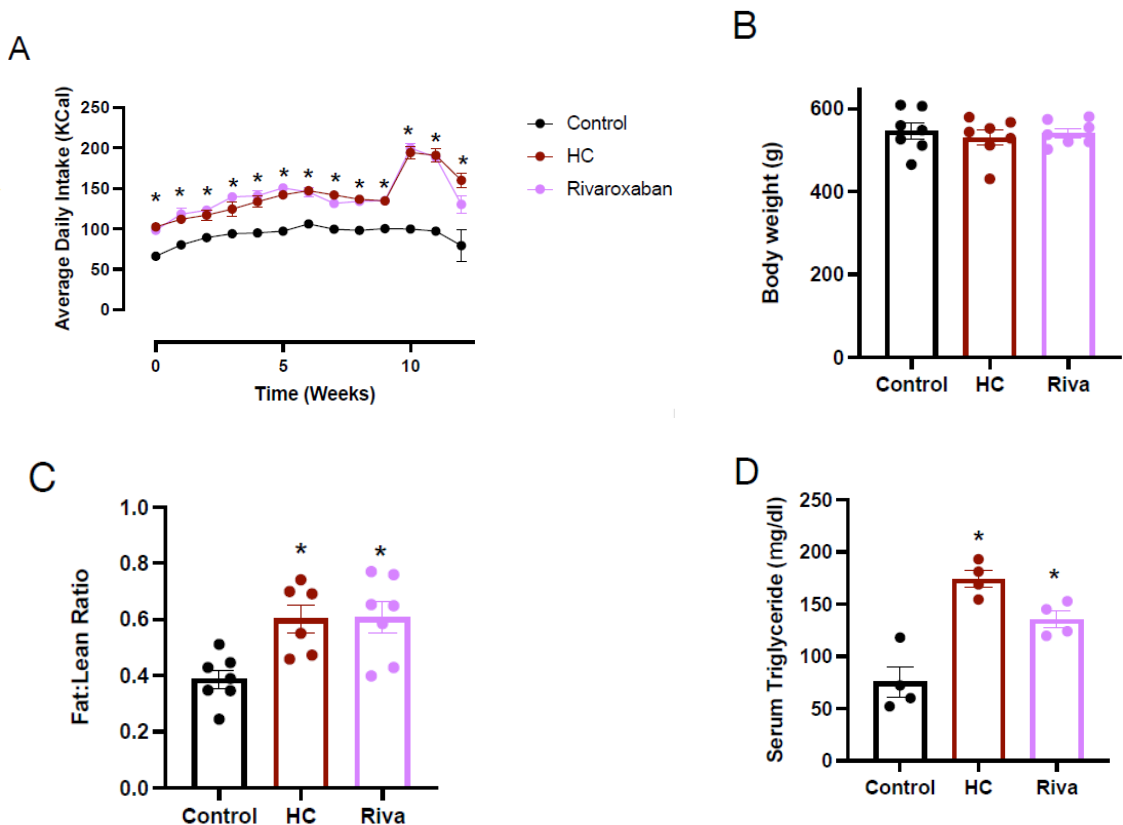


**Figure 2. Daily calorie intake and metabolic parameters of rats in different treatment groups.** A, Daily calorie intake in control versus HC-fed rats and rivaroxaban treated rats along the 12-week feeding duration (n=8). B, Body weight after 12-weeks of feeding for the three different groups (n=8). C, Body composition measured via NMR represented as fat:lean ratio for control versus HC-fed rats and rivaroxaban treated rats (n=8). D, Serum triglyceride measured after 12-weeks of feeding for the different treatment groups (n=4). Values are Mean  $\pm$  S.E.M. Statistical significance was tested using two-way ANOVA followed by Sidak's test (A) or one-way ANOVA followed by Tukey's multiple comparisons (B-D). \* denote  $P < 0.05$  versus corresponding values in control and HC-fed rats, respectively.

## **B. Baroreceptor Sensitivity with Single Treatments:**

### ***1. Cardiac (HR) and Vascular (MAP) Responses to Vasopressor, Phenylephrine***

The parasympathetic arm of the baroreflex was assessed using increasing doses of the vasoconstrictor PE separated by 5 minutes interval, and the subsequent bradycardic responses were examined. No significant difference in vasopressor effect in response to PE was noted between the three different groups (Fig. 3A). The decrease in HR ( $\Delta$  HR) seen with increasing doses of PE was lower in HC-fed rats compared to control rats (Fig. 3B). Moreover, the HC rats had a lower slope of linear regression of  $\Delta$  HR versus  $\Delta$  MAP confirming the presence of a blunted bradycardic response (Fig. 3C). It is worth noting that treatment with rivaroxaban significantly reversed the blunted BRS slope mounted by the HC-fed rats and set it to a value comparable to normal controls (Fig. 3 B, C, and D). Figure 4 depicts representative tracings of changes in MAP and HR in response to increasing doses of PE.

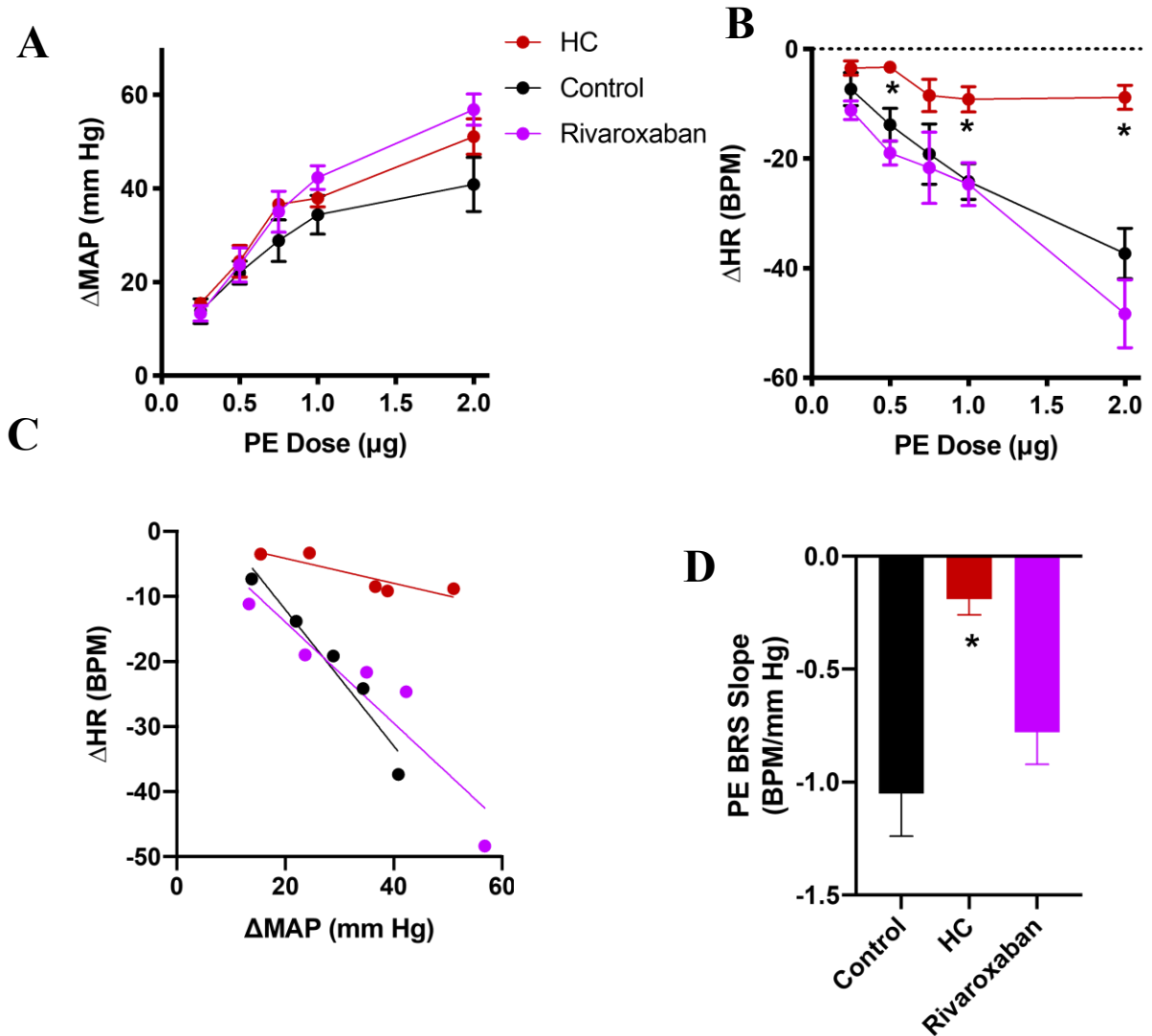


**Figure 3. The effect of HC feeding and treatment with rivaroxaban on the sensitivity of the parasympathetic arm of the baroreflex.** A, Pressor effect of different doses of PE in different groups (n=5). B, The reflex bradycardic response to increasing doses of PE. C, Best-fit regression lines for the correlation between changes in MAP in response to increasing PE doses and the reflex change in HR. D, Statistical comparison of the slopes of the best regression line of the  $\Delta$ MAP versus  $\Delta$ HR representing BRS in response to vasopressor PE doses. Values are Mean  $\pm$  S.E.M. Statistical significance was tested using two-way ANOVA followed by Sidak's test (A, B, C) or one-way ANOVA followed by Tukey's multiple comparisons (D). \* denote  $P < 0.05$  versus response at corresponding points in control.

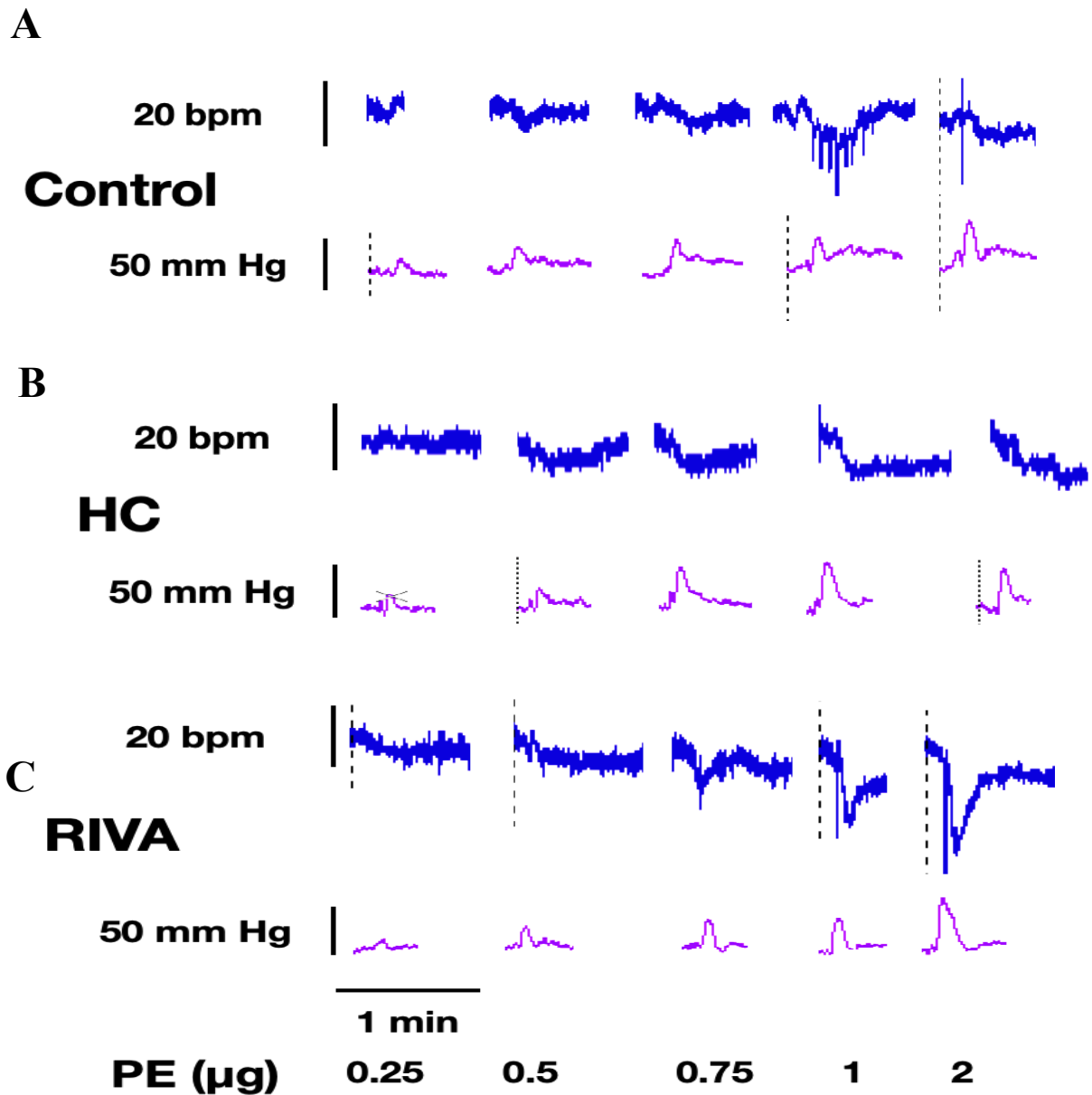


**Figure 4. Representative tracings of pressor [mean arterial pressure (MAP)] and cardiac [heart rate (HR)] responses to increasing doses of vasopressor phenylephrine (PE) in: A, Normal controls; B, HC-fed rats; C, rivaroxaban treated rats. Vertical scale bars represent MAP (50 mmHg) and HR [20 beats/min (BPM)], horizontal scale bars represent time (1 minute).**

## ***2. Cardiac (HR) and Vascular (MAP) Responses to Vasodilator, Sodium Nitroprusside***

The sympathetic arm of the baroreflex was assessed using increasing doses of the vasodepressor SNP separated by 5 minutes interval, and the subsequent tachycardic responses were examined. The steeper the regression lines' slope, the better was the functionality of the receptors. All prediabetic rats showed normal depressor responses to the various SNP's doses (Fig. 5A). Additionally, no change in the delta heart rate ( $\Delta$ HR) in response to SNP was observed (Fig. 5B). No differences in BRS in response to SNP was detected (Fig. 5C), which indicated that the reflex tachycardic response remained intact and was further confirmed by the lack of statistical significance of the different BRS slopes (Fig. 5D). Figure 6 depicts the representative tracing of changes in MAP and HR in response to increasing doses of SNP. The depressor responses induced by SNP remained unaltered in all groups confirming that the sympathetic system was not affected.

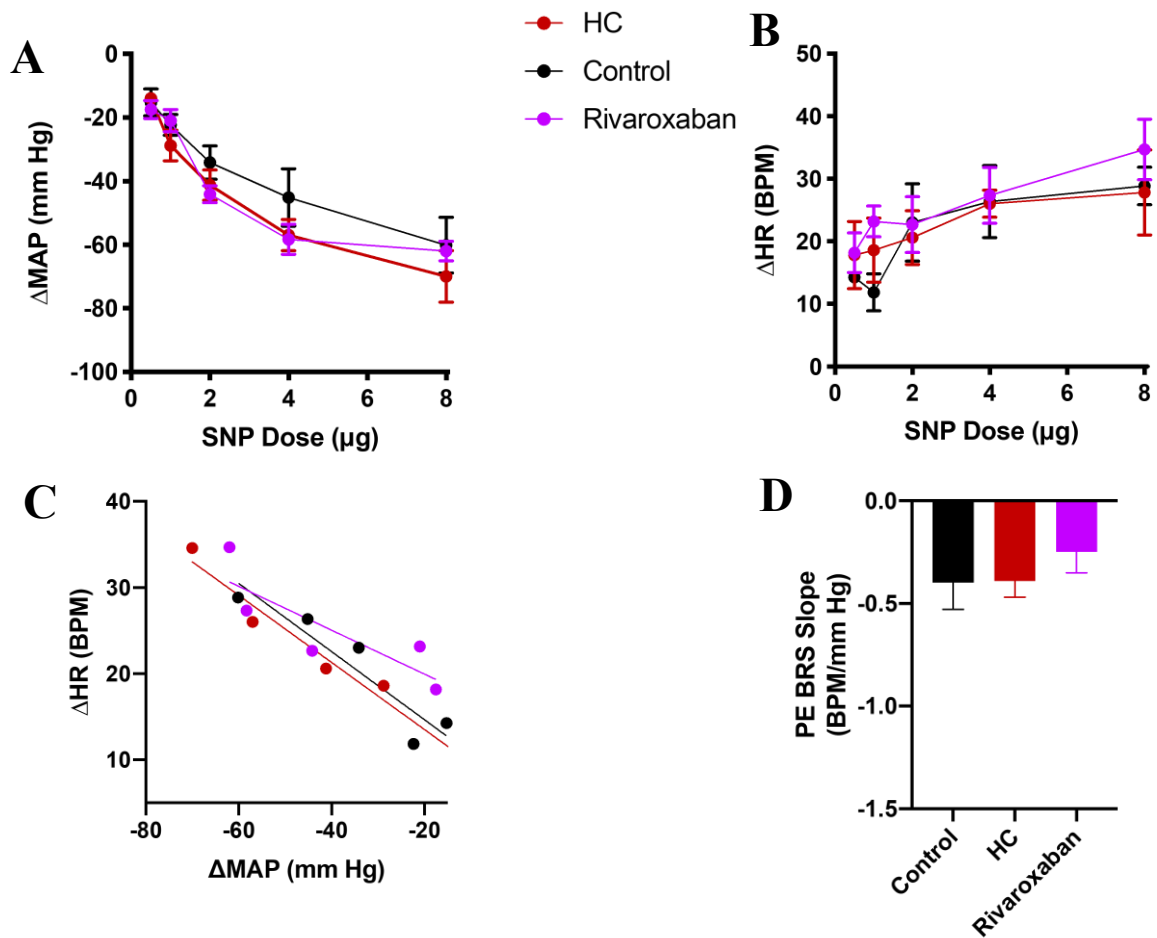


**Figure 5. The effect of HC feeding and treatment with rivaroxaban on the sensitivity of the sympathetic arm of the baroreflex.** A, Depressor effect of different doses of SNP in different groups (n=5). B, The reflex tachycardic responses to different doses of SNP. C, Best-fit regression lines for the correlation between changes in MAP in response to increasing SNP doses and the reflex change in HR. D, Statistical comparison of the slopes of the best regression line of the  $\Delta$ MAP versus  $\Delta$ HR in response to different SNP doses in different groups. Values are Mean  $\pm$  S.E.M. Statistical significance was tested using two-way ANOVA followed by Sidak's test (A, B, C) or one-way ANOVA followed by Tukey's multiple comparisons (D). \* denote  $P < 0.05$  versus response at corresponding points in control and HC groups respectively.

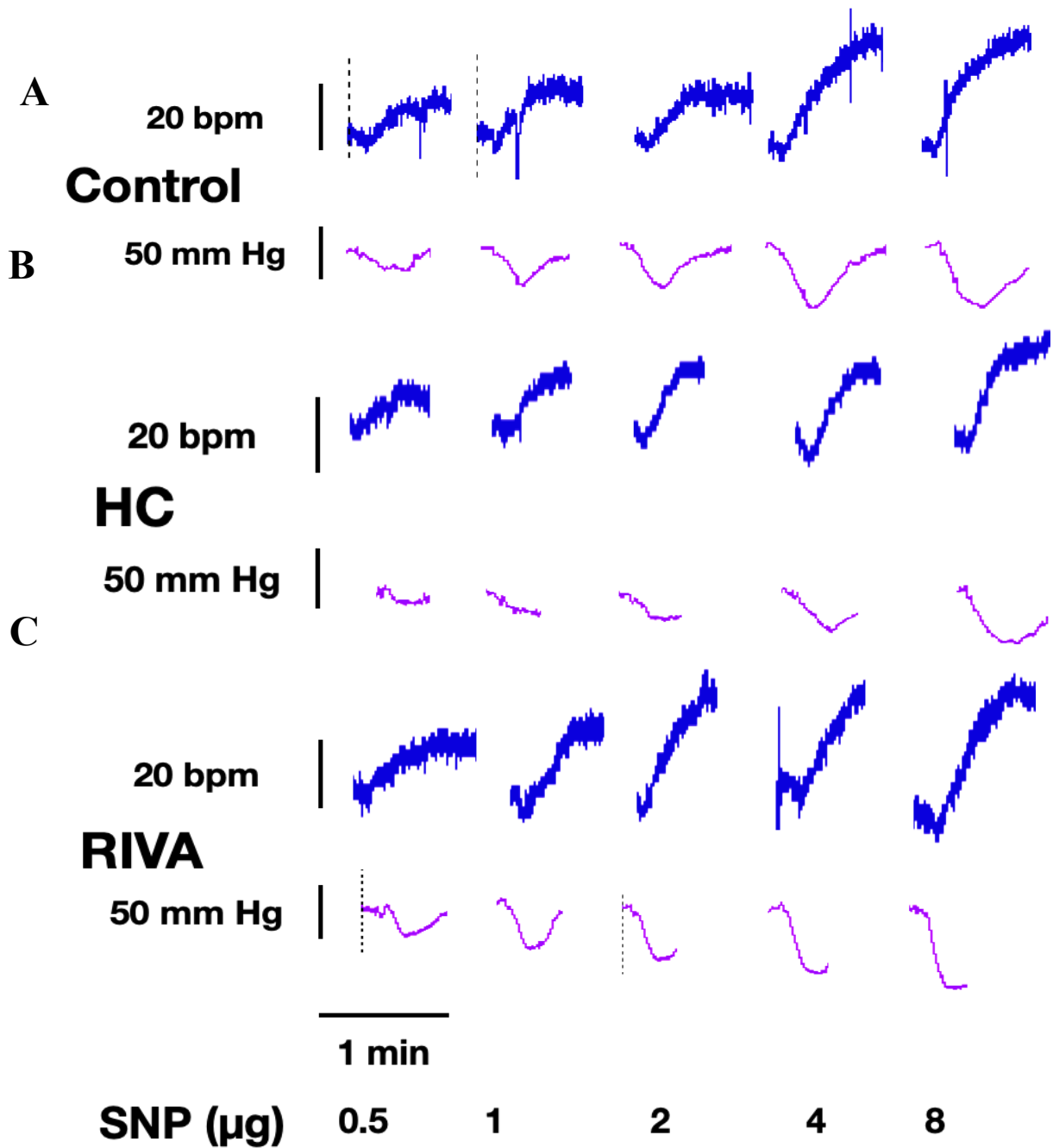


**Figure 6. Representative tracings of depressor [mean arterial pressure (MAP)] and cardiac [heart rate (HR)] responses to increasing doses of vasodilator sodium nitroprusside (SNP) in: A, Normal controls; B, HC-fed rats; C, rivaroxaban treated rats. Vertical scale bars represent MAP (50 mmHg) and HR [20 beats/min (BPM)], horizontal scale bars represent time (1 minute).**

### C. Impact of Rivaroxaban Treatment on PVAT Inflammation in HC-Fed Rats:

Previous studies reported an increased expression of inflammatory cytokines (TNF-  $\alpha$  and IL-1 $\beta$ ) in prediabetic rats, culminating in perivascular adipose tissue inflammation (55). Western blotting revealed that HC-fed rats expressed a marked increase in IL-1 $\beta$  expression, which was ameliorated by rivaroxaban treatment (Fig. 7).

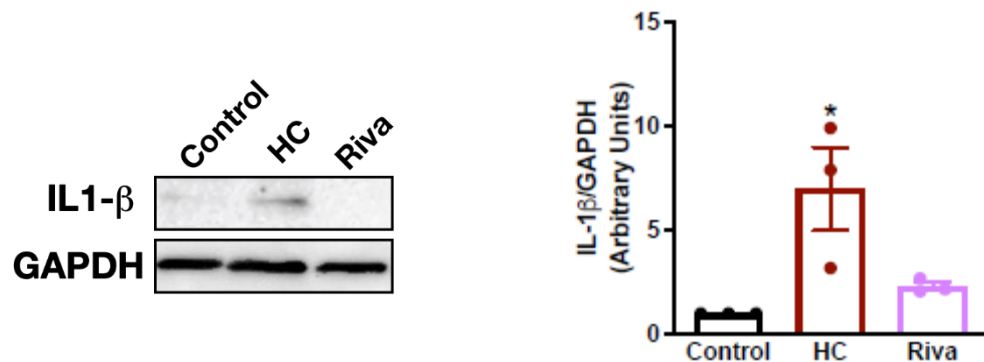


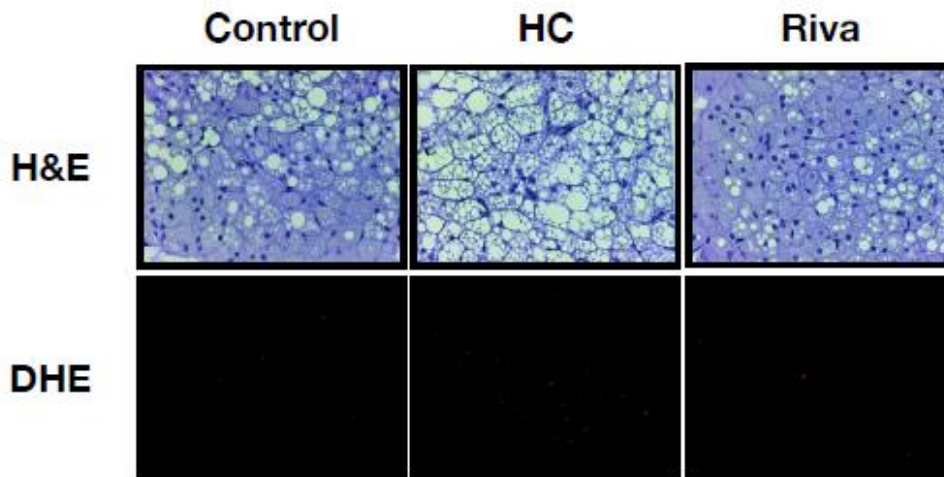
**Figure 7. The effect of HC feeding and treatment with rivaroxaban on inflammatory cytokine expression in perivascular adipose tissue.** Changes in IL-1 $\beta$  protein levels in perivascular adipose tissue, with a representative western blot. Depicted data represents Mean  $\pm$  S.E.M. Statistical significance was determined by one-way ANOVA followed by Tukey's *post hoc* test. \* denotes  $P < 0.05$  versus corresponding values in control.

### D. Impact of Rivaroxaban Treatment on PVAT Adipocyte Hypertrophy and Oxidative Stress in HC-Fed Rats:

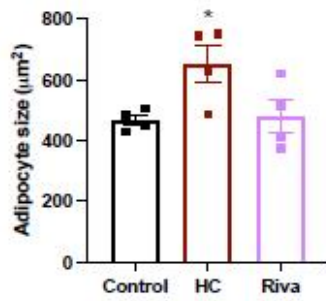
As expected, Hematoxylin and Eosin (H&E) staining indicated a significant increase in the perivascular adipocyte size of the HC-fed rats, further ameliorated by rivaroxaban treatment (Fig 8A). Furthermore, DHE staining revealed that HC-fed rats comprised a significant increase in oxidative stress in the PVAT, which was significantly reduced upon using rivaroxaban (Fig. 8B).



A



B



C

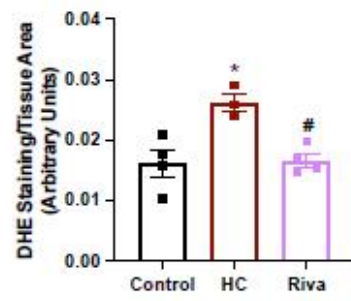


**Figure 8. The effect of mild hypercaloric diet and rivaroxaban treatment on PVAT size and oxidative stress.** A, Represents H&E staining of PVAT sections and the DHE staining intensity/tissue are exhibiting ROS (n=4). B, Represents the quantification of adipocyte size values. C, Represents the bar graph of DHE staining values. The red fluorescence represents DHE staining on the representative micrographs. Scale bars are 50  $\mu$ m. Depicted data represent Mean  $\pm$  S.E.M of results obtained from 12 slides from 4 different rats per group. Statistical significance was determined by one-way ANOVA followed by Tukey's post hoc test. \* and # denote P < 0.05 versus corresponding values in control and HC-fed rats, respectively.

### E. Impact of Rivaroxaban Treatment on Brainstem Oxidative Stress in HC-Fed Rats:

#### Rats:

As expected, DHE staining of brainstem cryosections showed elevated levels of ROS production in the brainstem of prediabetic rats. However, rivaroxaban treatment was not capable of reducing this significant elevation (Fig. 9).

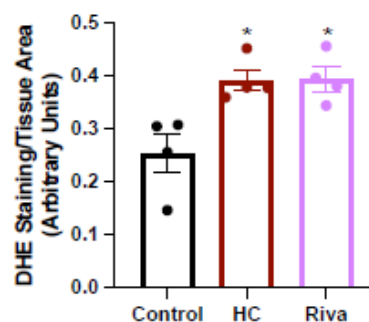
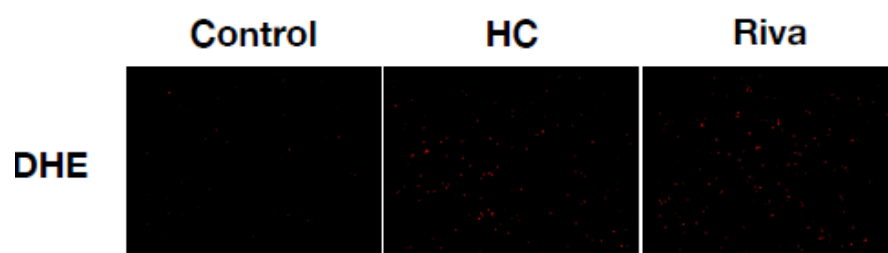


**Figure 9. The effect of mild hypercaloric diet and rivaroxaban treatment on brainstem oxidative stress.** Represents DHE staining of brainstem cryosections and its values represented in a bar graph of the three different groups (n=4). The red fluorescence represents DHE staining on the representative micrographs. Scale bars are 50  $\mu$ m. Depicted data represent Mean  $\pm$  S.E.M of results obtained from 12 slides from 4 different rats per group. Statistical significance was determined by one-way ANOVA followed by Tukey's *post hoc* test. \* denotes  $P < 0.05$  versus corresponding values in control.

## **F. Microscopic, Oxidative, and Inflammatory Changes in Ventricular Tissues:**

### **1. Hematoxylin and Eosin (H&E) Staining:**

H&E staining in the HC-fed rats' heart midsection tissues showed no significant difference in the area of interfibrillar edema in papillary muscle of the three different groups (Fig. 10 A, B).

### **2. Masson Trichrome Staining:**

Masson Trichrome staining reflected no change in the collagen deposition in the heart midsections of the three different groups (Fig. 10 A, C).

### **3. Dihydroethidium (DHE) Staining:**

Parallel with papillary muscle edema, DHE staining intensity/tissue area was significantly higher in the HC-fed rats. Interestingly, rivaroxaban treatment was capable of reducing this level (Fig. 10 A, D).

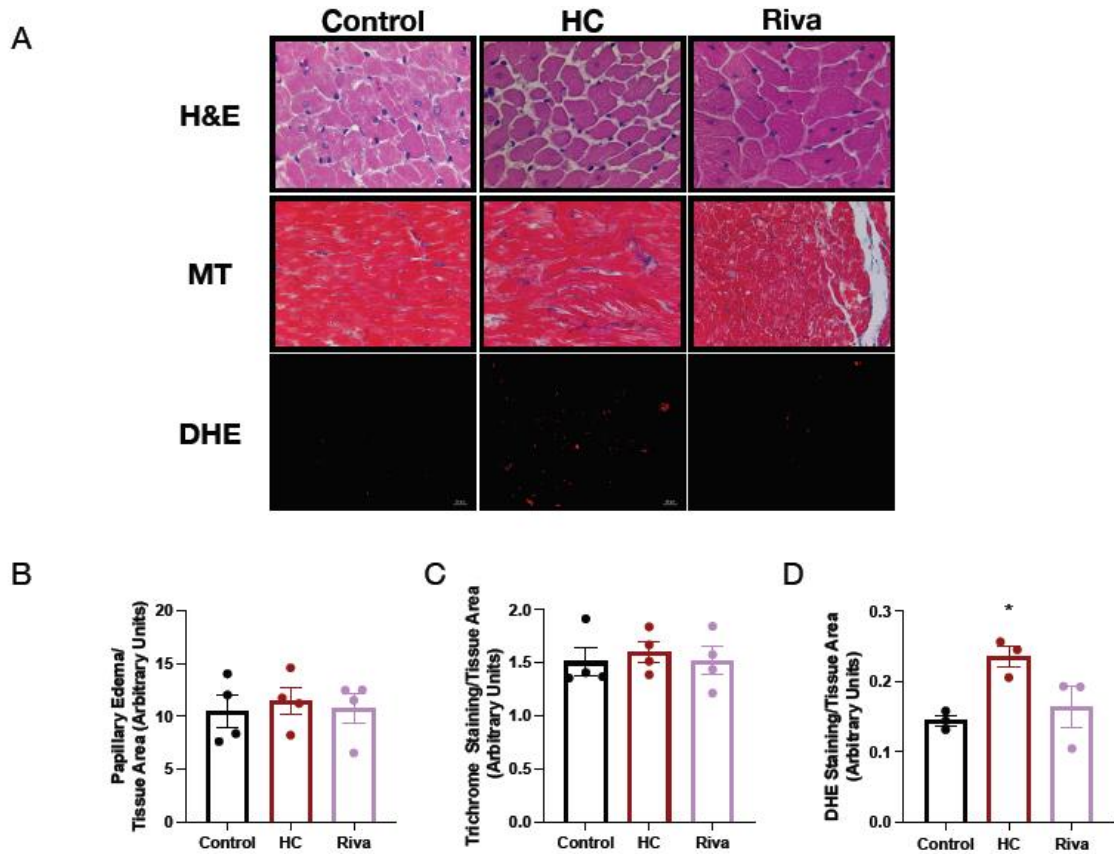


**Figure 10. Structural and molecular changes in ventricular tissue in response to HC feeding and rivaroxaban treatment.** A, Represents H&E stained micrographs of ventricular mid-sections showing transverse sections of the papillary muscle, Masson Trichrome stained micrographs of ventricular mid-sections, and DHE staining intensity of ventricular mid-sections. B, Represents bar graph H&E values of the interfibrillar edema. C, Represents the bar graph of Masson Trichrome values showing collagen staining. D, Represents the bar graph of DHE staining values showing ROS staining intensity (n=4). The red fluorescence represents DHE staining on the representative micrographs. Scale bars are 50  $\mu$ m. Depicted data represent Mean  $\pm$  S.E.M of results obtained from 12 slides from 4 different rats per group. Statistical significance was determined by one-way ANOVA followed by Tukey's *post hoc* test. \* denotes  $P < 0.05$  versus corresponding values in control.

## CHAPTER IV

### DISCUSSION

Diabetic patients present with already established cardiovascular disorders at initial diagnosis. Moreover, tight glycemic control is not enough to delay the progression indicating that cardiovascular disorders start early in the course of the disease with a pathogenesis rooted in the earlier prediabetic stage and possibly triggered by mechanisms other than hyperglycemia (65, 66). Indeed, the prediabetic stage was shown to be correlated with adipose tissue inflammation, ending up with cardiovascular diseases (67, 68). Among the early cardiovascular disorders that appear in prediabetic patients is the cardiac autonomic neuropathy (CAN) (67, 69). CAN is known as the impairment of the autonomic nerve fibers regulating the heart rate. It is a frequent chronic complication of diabetes accompanied with life threatening outcomes such as stroke, arrhythmias, myocardial ischemia, and CAD (44). Additionally, this early state of metabolic challenge is linked to a hypercoagulable state characterized by an increase in coagulation factor activity, such as tissue factor, factor Xa, and thrombin. Factor Xa, in particular, can act on PAR 1 and 2 further exacerbating adipose tissue inflammation, creating a stage known as thromboinflammation (27). In the present study, we showed that interruption of thromboinflammation by inhibition of factor Xa through rivaroxaban treatment ameliorated adipose inflammation and cardiac autonomic neuropathy in a rat model of early metabolic challenge.

To simulate the early metabolic insult in absence of hyperglycemia, a non-obese prediabetic rat model was used. This model received 38% of energy intake as fat, which is slightly above the ADA daily total fat intake recommendations (20-35%

energy as fat) (70), but within the lower range of high-fat diet compositions (20-60% energy as fat) used in validated rat models of obesity, insulin resistance, and diabetes (71). Refined sugars in the typical Western diet were also included in the rats' diet in the form of fructose. Thus, both high-fat and fructose feeding are necessary to develop the metabolic challenge in our rats (72). In previous studies from our laboratory, this rat model showed early metabolic impairment characterized by hyperinsulinemia, dyslipidemia, and adipose expansion and inflammation, which were correlated with early parasympathetic dysfunction (37). Indeed, the interventions that were able to mitigate adipose tissue inflammation, such as treatment with metformin and pioglitazone, were capable of reversing the early parasympathetic dysfunction (55).

In this study, we first showed that HC diet led to adipocytes expansion and elevation of serum lipids, without an increase in body weight. Interestingly, rivaroxaban did not affect these parameters indicating that any functional or structural effects observed in the rivaroxaban treated rats are not a result of indirect modulation of metabolic alterations. It is noteworthy, that PVAT inflammation manifesting as a significant rise in the cytokine IL-1 $\beta$  and ROS occurred concomitantly with the increase in adipocytes size. This structural change along with the inflammation was responsive to rivaroxaban treatment.

Additionally, cardiac autonomic function was assessed by baroreceptor sensitivity (BRS) testing, revealing an altered vagal control. In line with our previous study, a parasympathetic insult was evident and was reversed by rivaroxaban treatment. Specifically, HC-fed rats presented with a blunted bradycardiac response indicating the reduction in the cardiac vagal activity (55, 73). This vagal insult is consistent with increased brainstem oxidative stress. However, rivaroxaban treated rats did not show a

reduction in brainstem oxidative stress, which might be a result of its limited capacity to cross the blood brain barrier (BBB) (74-76). This might indicate that the origin of the vagal dysfunction is presumably peripheral in nature rather than central. Previous studies disclosed that type-2 diabetes leads to neuroinflammation due to the release of ROS and cytokines (73). Conversely, it is debatable whether ROS and cytokines are generated by microglial activation stimulated by hypoxia in the brain, or they gained access to the brain through the altered BBB (73, 77, 78). Importantly, since in this study ROS was increased in the brainstem, this indicates that neural inflammation might happen in the advanced stages of metabolic dysfunction after the worsening oxidative stress develops. Along the same lines, despite the lack of microscopic myocardial defects, the changes in ROS levels in HC-fed rats following rivaroxaban treatment reveal the rescues of an early molecular insult, that if not treated, might lead to cardiac structural deficits over time.

The contribution of thromboinflammation to adipose tissue inflammation induced cardiac autonomic neuropathy could be related to the action of factor Xa on PARs. PARs are not only present in adipose tissue, but also on cardiovascular cells (27, 79). A study done by Sabri et al. revealed that cardiomyocytes coexpress PARs 1 and 2 leading to hypertrophy and altered contractile function (79). Factor Xa was also shown to affect vascular smooth muscle cells (VSMCs) and endothelial cells (ECs) structure and function through PARs stimulation resulting in vascular remodeling, vascular injury, and atherosclerosis (27). Moreover, macrophages present in AT range from highly pro-inflammatory (M1) to highly anti-inflammatory (M2) that should be in balanced proportions (80, 81). Importantly, M1 macrophages are responsible for the secretion of pro-inflammatory cytokines as IL-1 $\beta$ . During metabolic dysfunction, M1

macrophages become in excess resulting in increased tissue inflammation (80, 81). A study done by Zuo et al. illustrated that factor Xa acts on macrophages through PAR 2 to enhance the expression of pro-inflammatory cytokines (82). As such, rivaroxaban might have been able to ameliorate cardiac autonomic neuropathy by directly affecting the cardiovascular structure and function through decreasing vascular inflammation (83), or by affecting macrophages expressing PARs and triggering adipose tissue inflammation (84).

In conclusion, although rivaroxaban was not capable of reversing the metabolic dysfunction, it was capable of interrupting thromboinflammation and ameliorating adipose tissue inflammation, which eventually might have improved the baroreceptor sensitivity and mitigated CAN.



## CHAPTER V

### LIMITATIONS AND FUTURE DIRECTIONS

The present study has several limitations. First, the safety profile of rivaroxaban dose and the anticoagulant side effects resulting in non-thromboembolic disorders need to be established in control rats so that one can infer the appropriate dose to be used. Second, our work was done on male rats only. In fact, gender plays a major role in experimental results; as such, female rats should be tested as females acquire variable large subcutaneous fat depots and hormones, contributing to different rivaroxaban treatment responses. Thus, we aim to allocate new batches of female rats to investigate the outcomes. Third, further investigation regarding the relationship between PARs or factor Xa and PVAT inflammation should be assessed in the future using PARs antagonists or western blotting for factor Xa in PVAT to detect the definitive involvement of both factors in the vicious cycle. Fourth, immune cells like macrophages were shown in previous studies to be involved in promoting thromboinflammation which we did not study here. Hence, we aim to study using flow-cytometry the mechanism of action in which macrophages mediate thromboinflammation. Finally, the lack of necessary control groups force us to raise up more rats such as control rats treated with rivaroxaban, and rats on normal chow consuming fructose water with and without rivaroxaban treatment, these two groups will act as controls so we can compare to and reach valid results.

## REFERENCES

1. Saeedi P, Salpea P, Karuranga S, Petersohn I, Malanda B, Gregg EW, et al. Mortality attributable to diabetes in 20-79 years old adults, 2019 estimates: Results from the International Diabetes Federation Diabetes Atlas, 9(th) edition. *Diabetes Res Clin Pract.* 2020;162:108086.
2. WHO. Diabetes. 2019.
3. IDF. Diabetes Atlas 9th Edition. 2019.
4. American Diabetes A. Diagnosis and classification of diabetes mellitus. *Diabetes Care.* 2014;37 Suppl 1:S81-90.
5. American Diabetes A. 2. Classification and Diagnosis of Diabetes: Standards of Medical Care in Diabetes-2020. *Diabetes Care.* 2020;43(Suppl 1):S14-S31.
6. Papatheodorou K, Banach M, Bekiari E, Rizzo M, Edmonds M. Complications of Diabetes 2017. *J Diabetes Res.* 2018;2018:3086167.
7. Bansal N. Prediabetes diagnosis and treatment: A review. *World J Diabetes.* 2015;6(2):296-303.
8. Prevention CfDCA. Prediabetes-Your Chance to Prevent Type 2 Diabetes. 2020.
9. Wilson ML. Prediabetes: Beyond the Borderline. *Nurs Clin North Am.* 2017;52(4):665-77.
10. Weir GC, Bonner-Weir S. Five stages of evolving beta-cell dysfunction during progression to diabetes. *Diabetes.* 2004;53 Suppl 3:S16-21.
11. Tabak AG, Herder C, Rathmann W, Brunner EJ, Kivimaki M. Prediabetes: a high-risk state for diabetes development. *Lancet.* 2012;379(9833):2279-90.
12. Sorensen BM, Houben AJ, Berendschot TT, Schouten JS, Kroon AA, van der Kallen CJ, et al. Prediabetes and Type 2 Diabetes Are Associated With Generalized Microvascular Dysfunction: The Maastricht Study. *Circulation.* 2016;134(18):1339-52.
13. Edwards CM, Cusi K. Prediabetes: A Worldwide Epidemic. *Endocrinol Metab Clin North Am.* 2016;45(4):751-64.
14. Vaskovic J. Adipose Tissue: Definition, location, function. 2021.
15. Kershaw EE, Flier JS. Adipose tissue as an endocrine organ. *J Clin Endocrinol Metab.* 2004;89(6):2548-56.
16. Coelho M, Oliveira T, Fernandes R. Biochemistry of adipose tissue: an endocrine organ. *Arch Med Sci.* 2013;9(2):191-200.
17. Qi XY, Qu SL, Xiong WH, Rom O, Chang L, Jiang ZS. Perivascular adipose tissue (PVAT) in atherosclerosis: a double-edged sword. *Cardiovasc Diabetol.* 2018;17(1):134.
18. Fitzgibbons TP, Czech MP. Epicardial and perivascular adipose tissues and their influence on cardiovascular disease: basic mechanisms and clinical associations. *J Am Heart Assoc.* 2014;3(2):e000582.
19. Wu J, Bostrom P, Sparks LM, Ye L, Choi JH, Giang AH, et al. Beige adipocytes are a distinct type of thermogenic fat cell in mouse and human. *Cell.* 2012;150(2):366-76.
20. Grigoras A, Balan RA, Caruntu ID, Giusca SE, Lozaneanu L, Avadanei RE, et al. Perirenal Adipose Tissue-Current Knowledge and Future Opportunities. *J Clin Med.* 2021;10(6).
21. Britton KA, Fox CS. Perivascular adipose tissue and vascular disease. *Clin Lipidol.* 2011;6(1):79-91.

22. Brown NK, Zhou Z, Zhang J, Zeng R, Wu J, Eitzman DT, et al. Perivascular adipose tissue in vascular function and disease: a review of current research and animal models. *Arterioscler Thromb Vasc Biol.* 2014;34(8):1621-30.
23. Kim HW, Belin de Chantemele EJ, Weintraub NL. Perivascular Adipocytes in Vascular Disease. *Arterioscler Thromb Vasc Biol.* 2019;39(11):2220-7.
24. Rafeh R, Viveiros A, Oudit GY, El-Yazbi AF. Targeting perivascular and epicardial adipose tissue inflammation: therapeutic opportunities for cardiovascular disease. *Clin Sci (Lond).* 2020;134(7):827-51.
25. Donath MY, Shoelson SE. Type 2 diabetes as an inflammatory disease. *Nat Rev Immunol.* 2011;11(2):98-107.
26. Elkhatib MAW, Mroueh A, Rafeh RW, Sleiman F, Fouad H, Saad EI, et al. Amelioration of perivascular adipose inflammation reverses vascular dysfunction in a model of nonobese prediabetic metabolic challenge: potential role of antidiabetic drugs. *Transl Res.* 2019;214:121-43.
27. Alaaeddine RA, AlZaim I, Hammoud SH, Arakji A, Eid AH, Abd-Elrahman KS, et al. The pleiotropic effects of antithrombotic drugs in the metabolic-cardiovascular-neurodegenerative disease continuum: impact beyond reduced clotting. *Clin Sci (Lond).* 2021;135(8):1015-51.
28. Winter WE, Greene DN, Beal SG, Isom JA, Manning H, Wilkerson G, et al. Clotting factors: Clinical biochemistry and their roles as plasma enzymes. *Adv Clin Chem.* 2020;94:31-84.
29. Smith SA, Travers RJ, Morrissey JH. How it all starts: Initiation of the clotting cascade. *Crit Rev Biochem Mol Biol.* 2015;50(4):326-36.
30. Pasma JJ, Grover SP, Hisada Y, Owens AP, 3rd, Antoniak S, Spronk HM, et al. Roles of Coagulation Proteases and PARs (Protease-Activated Receptors) in Mouse Models of Inflammatory Diseases. *Arterioscler Thromb Vasc Biol.* 2019;39(1):13-24.
31. Pasma JJ, Posthuma JJ, Spronk HM. Coagulation and non-coagulation effects of thrombin. *J Thromb Haemost.* 2016;14(10):1908-16.
32. Ruf W, Samad F. Tissue factor pathways linking obesity and inflammation. *Hamostaseologie.* 2015;35(3):279-83.
33. Vinik AI, Erbas T, Casellini CM. Diabetic cardiac autonomic neuropathy, inflammation and cardiovascular disease. *J Diabetes Investig.* 2013;4(1):4-18.
34. Pop-Busui R. Cardiac autonomic neuropathy in diabetes: a clinical perspective. *Diabetes Care.* 2010;33(2):434-41.
35. Vinik AI, Casellini C, Parson HK, Colberg SR, Nevoret ML. Cardiac Autonomic Neuropathy in Diabetes: A Predictor of Cardiometabolic Events. *Front Neurosci.* 2018;12:591.
36. Serhiyenko VA, Serhiyenko AA. Cardiac autonomic neuropathy: Risk factors, diagnosis and treatment. *World J Diabetes.* 2018;9(1):1-24.
37. Bakkar NZ, Dwaib HS, Fares S, Eid AH, Al-Dhaheri Y, El-Yazbi AF. Cardiac Autonomic Neuropathy: A Progressive Consequence of Chronic Low-Grade Inflammation in Type 2 Diabetes and Related Metabolic Disorders. *Int J Mol Sci.* 2020;21(23).
38. Dimitropoulos G, Tahrani AA, Stevens MJ. Cardiac autonomic neuropathy in patients with diabetes mellitus. *World J Diabetes.* 2014;5(1):17-39.
39. Kuehl M, Stevens MJ. Cardiovascular autonomic neuropathies as complications of diabetes mellitus. *Nat Rev Endocrinol.* 2012;8(7):405-16.

40. McCorry LK. Physiology of the autonomic nervous system. *Am J Pharm Educ.* 2007;71(4):78.
41. Tarvainen MP, Laitinen TP, Lipponen JA, Cornforth DJ, Jelinek HF. Cardiac autonomic dysfunction in type 2 diabetes - effect of hyperglycemia and disease duration. *Front Endocrinol (Lausanne).* 2014;5:130.
42. Levick JR. Cardiovascular receptors, reflexes, and central control. *An introduction to Cardiovascular Physiology.* 2003:279-96.
43. Crisafulli A, Marongiu E, Ogoh S. Cardiovascular Reflexes Activity and Their Interaction during Exercise. *Biomed Res Int.* 2015;2015:394183.
44. Bissinger A. Cardiac Autonomic Neuropathy: Why Should Cardiologists Care about That? *J Diabetes Res.* 2017;2017:5374176.
45. Peng CK, Havlin S, Stanley HE, Goldberger AL. Quantification of scaling exponents and crossover phenomena in nonstationary heartbeat time series. *Chaos.* 1995;5(1):82-7.
46. La Rovere MT, Pinna GD, Raczak G. Baroreflex sensitivity: measurement and clinical implications. *Ann Noninvasive Electrocardiol.* 2008;13(2):191-207.
47. Porth CJ, Bamrah VS, Tristani FE, Smith JJ. The Valsalva maneuver: mechanisms and clinical implications. *Heart Lung.* 1984;13(5):507-18.
48. Manzella D, Paolisso G. Cardiac autonomic activity and Type II diabetes mellitus. *Clin Sci (Lond).* 2005;108(2):93-9.
49. Keyl C, Lemberger P, Palitzsch KD, Hochmuth K, Liebold A, Hobbhahn J. Cardiovascular autonomic dysfunction and hemodynamic response to anesthetic induction in patients with coronary artery disease and diabetes mellitus. *Anesth Analg.* 1999;88(5):985-91.
50. Lieb DC, Parson HK, Mamikunian G, Vinik AI. Cardiac autonomic imbalance in newly diagnosed and established diabetes is associated with markers of adipose tissue inflammation. *Exp Diabetes Res.* 2012;2012:878760.
51. Thiyagarajan R, Subramanian SK, Sampath N, Madanmohan T, Pal P, Bobby Z, et al. Association between cardiac autonomic function, oxidative stress and inflammatory response in impaired fasting glucose subjects: cross-sectional study. *PLoS One.* 2012;7(7):e41889.
52. Wakabayashi S, Aso Y. Adiponectin concentrations in sera from patients with type 2 diabetes are negatively associated with sympathovagal balance as evaluated by power spectral analysis of heart rate variation. *Diabetes Care.* 2004;27(10):2392-7.
53. Cooper TM, McKinley PS, Seeman TE, Choo TH, Lee S, Sloan RP. Heart rate variability predicts levels of inflammatory markers: Evidence for the vagal anti-inflammatory pathway. *Brain Behav Immun.* 2015;49:94-100.
54. Fox CS, Golden SH, Anderson C, Bray GA, Burke LE, de Boer IH, et al. Update on Prevention of Cardiovascular Disease in Adults With Type 2 Diabetes Mellitus in Light of Recent Evidence: A Scientific Statement From the American Heart Association and the American Diabetes Association. *Diabetes Care.* 2015;38(9):1777-803.
55. Al-Assi O, Ghali R, Mroueh A, Kaplan A, Mougharbil N, Eid AH, et al. Cardiac Autonomic Neuropathy as a Result of Mild Hypercaloric Challenge in Absence of Signs of Diabetes: Modulation by Antidiabetic Drugs. *Oxid Med Cell Longev.* 2018;2018:9389784.
56. Di Minno A, Frigerio B, Spadarella G, Ravani A, Sansaro D, Amato M, et al. Old and new oral anticoagulants: Food, herbal medicines and drug interactions. *Blood Rev.* 2017;31(4):193-203.

57. Mueck W, Stampfuss J, Kubitzka D, Becka M. Clinical pharmacokinetic and pharmacodynamic profile of rivaroxaban. *Clin Pharmacokinet.* 2014;53(1):1-16.
58. Trujillo T, Dobesh PP. Clinical use of rivaroxaban: pharmacokinetic and pharmacodynamic rationale for dosing regimens in different indications. *Drugs.* 2014;74(14):1587-603.
59. Chen A, Stecker E, B AW. Direct Oral Anticoagulant Use: A Practical Guide to Common Clinical Challenges. *J Am Heart Assoc.* 2020;9(13):e017559.
60. Mekaj YH, Mekaj AY, Duci SB, Miftari EI. New oral anticoagulants: their advantages and disadvantages compared with vitamin K antagonists in the prevention and treatment of patients with thromboembolic events. *Ther Clin Risk Manag.* 2015;11:967-77.
61. Spronk HM, de Jong AM, Crijns HJ, Schotten U, Van Gelder IC, Ten Cate H. Pleiotropic effects of factor Xa and thrombin: what to expect from novel anticoagulants. *Cardiovasc Res.* 2014;101(3):344-51.
62. Hashikata T, Yamaoka-Tojo M, Namba S, Kitasato L, Kameda R, Murakami M, et al. Rivaroxaban Inhibits Angiotensin II-Induced Activation in Cultured Mouse Cardiac Fibroblasts Through the Modulation of NF-kappaB Pathway. *Int Heart J.* 2015;56(5):544-50.
63. Zhou Q, Bea F, Preusch M, Wang H, Isermann B, Shahzad K, et al. Evaluation of plaque stability of advanced atherosclerotic lesions in apo E-deficient mice after treatment with the oral factor Xa inhibitor rivaroxaban. *Mediators Inflamm.* 2011;2011:432080.
64. Wu H, Ballantyne CM. Metabolic Inflammation and Insulin Resistance in Obesity. *Circ Res.* 2020;126(11):1549-64.
65. Kishore P, Kim SH, Crandall JP. Glycemic control and cardiovascular disease: what's a doctor to do? *Curr Diab Rep.* 2012;12(3):255-64.
66. Leon BM, Maddox TM. Diabetes and cardiovascular disease: Epidemiology, biological mechanisms, treatment recommendations and future research. *World J Diabetes.* 2015;6(13):1246-58.
67. Huang Y, Cai X, Mai W, Li M, Hu Y. Association between prediabetes and risk of cardiovascular disease and all cause mortality: systematic review and meta-analysis. *BMJ.* 2016;355:i5953.
68. Berezin AE, Berezin AA, Lichtenauer M. Emerging Role of Adipocyte Dysfunction in Inducing Heart Failure Among Obese Patients With Prediabetes and Known Diabetes Mellitus. *Front Cardiovasc Med.* 2020;7:583175.
69. Balcioglu AS, Akinci S, Cicek D, Eldem HO, Coner A, Bal UA, et al. Which is responsible for cardiac autonomic dysfunction in non-diabetic patients with metabolic syndrome: Prediabetes or the syndrome itself? *Diabetes Metab Syndr.* 2016;10(1 Suppl 1):S13-20.
70. Evert AB, Boucher JL, Cypress M, Dunbar SA, Franz MJ, Mayer-Davis EJ, et al. Nutrition therapy recommendations for the management of adults with diabetes. *Diabetes Care.* 2013;36(11):3821-42.
71. Buettner R, Scholmerich J, Bollheimer LC. High-fat diets: modeling the metabolic disorders of human obesity in rodents. *Obesity (Silver Spring).* 2007;15(4):798-808.
72. Lozano I, Van der Werf R, Bietiger W, Seyfritz E, Peronet C, Pinget M, et al. High-fructose and high-fat diet-induced disorders in rats: impact on diabetes risk, hepatic and vascular complications. *Nutr Metab (Lond).* 2016;13:15.

73. Bakkar NZ, Mougharbil N, Mroueh A, Kaplan A, Eid AH, Fares S, et al. Worsening baroreflex sensitivity on progression to type 2 diabetes: localized vs. systemic inflammation and role of antidiabetic therapy. *Am J Physiol Endocrinol Metab.* 2020;319(5):E835-E51.
74. Ru San T, Chan MY, Wee Siong T, Kok Foo T, Kheng Siang N, Lee SH, et al. Stroke prevention in atrial fibrillation: understanding the new oral anticoagulants dabigatran, rivaroxaban, and apixaban. *Thrombosis.* 2012;2012:108983.
75. Ploen R, Sun L, Zhou W, Heitmeier S, Zorn M, Jenetzky E, et al. Rivaroxaban does not increase hemorrhage after thrombolysis in experimental ischemic stroke. *J Cereb Blood Flow Metab.* 2014;34(3):495-501.
76. M. R. Molecular structure, lipophilicity, solubility, absorption, and polar surface area of novel anticoagulant agents. 2009;916:76-85.
77. Chen R, Lai UH, Zhu L, Singh A, Ahmed M, Forsyth NR. Reactive Oxygen Species Formation in the Brain at Different Oxygen Levels: The Role of Hypoxia Inducible Factors. *Front Cell Dev Biol.* 2018;6:132.
78. Van Dyken P, Lacoste B. Impact of Metabolic Syndrome on Neuroinflammation and the Blood-Brain Barrier. *Front Neurosci.* 2018;12:930.
79. Sabri A, Muske G, Zhang H, Pak E, Darrow A, Andrade-Gordon P, et al. Signaling properties and functions of two distinct cardiomyocyte protease-activated receptors. *Circ Res.* 2000;86(10):1054-61.
80. Ruggiero AD, Key CC, Kavanagh K. Adipose Tissue Macrophage Polarization in Healthy and Unhealthy Obesity. *Front Nutr.* 2021;8:625331.
81. Lim J, Iyer A, Liu L, Suen JY, Lohman RJ, Seow V, et al. Diet-induced obesity, adipose inflammation, and metabolic dysfunction correlating with PAR2 expression are attenuated by PAR2 antagonism. *FASEB J.* 2013;27(12):4757-67.
82. Zuo P, Zuo Z, Wang X, Chen L, Zheng Y, Ma G, et al. Factor Xa induces pro-inflammatory cytokine expression in RAW 264.7 macrophages via protease-activated receptor-2 activation. *Am J Transl Res.* 2015;7(11):2326-34.
83. Coughlin SR. Thrombin signalling and protease-activated receptors. *Nature.* 2000;407(6801):258-64.
84. Rayees S, Rochford I, Joshi JC, Joshi B, Banerjee S, Mehta D. Macrophage TLR4 and PAR2 Signaling: Role in Regulating Vascular Inflammatory Injury and Repair. *Front Immunol.* 2020;11:2091.